Constructing chaotic coordinates for HINT2 calculations

Stuart R. Hudson & Yasuhiro Suzuki

Princeton Plasma Physics Laboratory, U.S.A.
National Institute for Fusion Science, Japan

Introduction

Understanding the structure of chaotic magnetic fields is important for understanding confinement in 3D devices
(magnetic islands, “good” flux surfaces = KAM surfaces, “broken” flux surfaces = cantori, chaotic field lines, . . .)

Even for non-integrable fields, straight fieldline (i.e. action-angle) coordinates ***can*** be constructed on the invariant sets, e.g. the periodic orbits
(the irrational invariant sets, i.e. the KAM surfaces & cantori, can be closely approximated by periodic orbits)

Chaotic coordinates are based on a selection of “almost-invariant” quadratic-flux minimizing (QFM) surfaces.

In chaotic coordinates, the chaotic structure of the magnetic field is revealed, the flux surfaces are straight and the islands are “square”.

The magnetic field is given in cylindrical coordinates, and arbitrary, toroidal coordinates are introduced.

$$
\begin{aligned}
R &= R(\rho,\theta,\zeta) = \textstyle\sum_{m,n} R_{m,n}(\rho)\cos(m\theta - n\zeta) \\
\phi &= \zeta \\
Z &= Z(\rho,\theta,\zeta) = \textstyle\sum_{m,n} Z_{m,n}(\rho)\sin(m\theta - n\zeta)
\end{aligned}
$$

$$
\mathbf{B} = B^R\mathbf{e}_R + B^\phi\mathbf{e}_\phi + B^Z\mathbf{e}_Z = B^\rho\mathbf{e}_\rho + B^\theta\mathbf{e}_\theta + B^\zeta\mathbf{e}_\zeta
$$

$$
\begin{pmatrix} B^R \\ B^\phi \\ B^Z \end{pmatrix} = \begin{pmatrix} R_\rho & R_\theta & R_\zeta \\ \phi_\rho & \phi_\theta & \phi_\zeta \\ Z_\rho & Z_\theta & Z_\zeta \end{pmatrix} \begin{pmatrix} B^\rho \\ B^\theta \\ B^\zeta \end{pmatrix}
$$

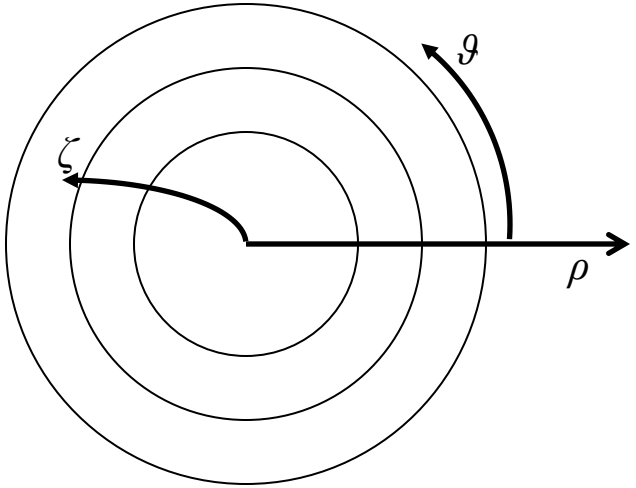

Begin with circular cross section coordinates, centered on the magnetic axis.

In practice, we will have a discrete set of toroidal surfaces that will be used as coordinate surfaces.

The Fourier harmonics, $R_{m,n}$ & $Z_{m,n}$, of the toroidal surfaces are interpolated using cubic/quintic polynomials.

(if the surfaces are smooth and well separated, this "simple-minded" interpolation works.)

A regularization factor is introduced, e.g. $R_{m,n}(\rho) = \rho^{m/2}\bar{X}_{m,n}(\rho) + R_{m,n}(0)$
to ensure that the interpolated surfaces do not overlap near the coordinate origin=magnetic axis.

A magnetic vector potential, in a suitable gauge, is quickly determined by radial integration.

$$\mathbf{A} = A_\theta(\rho,\theta,\zeta)\nabla\theta + A_\zeta(\rho,\theta,\zeta)\nabla\zeta$$

$$\begin{aligned}
\sqrt{g}B^\rho &= \partial_\theta A_\zeta - \partial_\zeta A_\theta \\
\sqrt{g}B^\theta &= -\partial_\rho A_\zeta \\
\sqrt{g}B^\zeta &= \partial_\rho A_\theta
\end{aligned}$$

$$\begin{aligned}
\partial_\rho A_{\theta,m,n} &= (\sqrt{g}B^\zeta)_{m,n} \\
\partial_\rho A_{\zeta,m,n} &= -(\sqrt{g}B^\theta)_{m,n}
\end{aligned}$$

hereafter, we will use the notation $\mathbf{A} \equiv \psi\nabla\theta - \chi\nabla\zeta$

ψ is the toroidal flux, and χ is called the magnetic field-line Hamiltonian

The magnetic fieldline action is the line integral of the vector potential

$S = \int_C \mathbf{A} \cdot d\mathbf{l}$, along an arbitrary trial-curve C, $\rho(\zeta)$, $\vartheta(\zeta)$.

$A = \psi \nabla\vartheta - \chi \nabla\zeta$,

$\psi = \sum \psi_{mn}(\rho)\cos(m\vartheta - n\zeta), \quad \chi = \sum \chi_{mn}(\rho)\cos(m\vartheta - n\zeta)$

Numerically, a curve is represented as a piecewise-constant, piecewise-linear.

piecewise-constant, piecewise-linear

For $\zeta \in (\zeta_{i-1}, \zeta_i)$

$$\rho(\zeta) = \rho_i$$
$$\theta(\zeta) = \theta_{i-1} + \dot{\theta} \quad (\zeta - \zeta_{i-1})$$

where $\dot{\theta} \equiv (\theta_i - \theta_{i-1})/\Delta\zeta$ is constant,

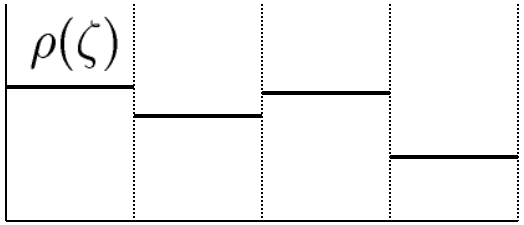

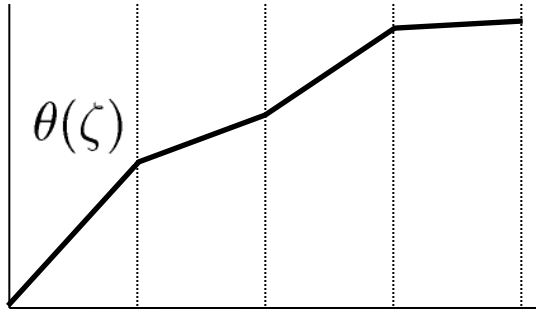

$$S \equiv \sum_{i=1}^{N} \int_{\zeta_{i-1}}^{\zeta_i} d\zeta \ \mathbf{A} \cdot d\mathbf{l} \equiv \sum_{i=1}^{N} \sum_{m,n} \left[\psi_{mn}(\rho_i)\ \dot{\theta} - \chi_{mn}(\rho_i)\right] \int_{\zeta_{i-1}}^{\zeta_i} d\zeta \cos(m\theta - n\zeta)$$

the integrals are evaluated analytically, ***i.e. method is FAST***

$$\int_{\zeta_{i-1}}^{\zeta_i} d\zeta \ \cos(m\theta - n\zeta) = \frac{\sin(m\theta_i - n\zeta_i) - \sin(m\theta_{i-1} - n\zeta_{i-1})}{m\dot{\theta} - n}$$

The derivatives of the magnetic fieldline action give the equations defining magnetic fieldlines

- $\delta S = \int_C \left[\delta\vartheta \frac{\partial S}{\partial \vartheta} + \delta\rho \frac{\partial S}{\partial \rho} \right] \mathbf{.dl}$, where $\frac{\partial S}{\partial \vartheta} = \sqrt{g} B^{\rho} - \dot{\rho}\sqrt{g} B^{\zeta}$ and $\frac{\partial S}{\partial \rho} = \dot{\vartheta}\sqrt{g} B^{\zeta} - \sqrt{g} B^{\vartheta}$

The construction of extremal curves of the action can be generalized to extremal surfaces of the quadratic flux.

- Introduce (i) a surface, $\rho \equiv \mathrm{P}(\vartheta,\zeta)$, and on the surface

  draw (ii) a family of periodic trial-curves, $\vartheta_\alpha(\zeta) \equiv \alpha + p\zeta / q + \tilde{\vartheta}_\alpha(\zeta)$

- We can choose $\frac{\partial S}{\partial \rho} = 0$, i.e. $\dot{\vartheta} = B^{\vartheta} / B^{\zeta}$, but generally $\frac{\partial S}{\partial \vartheta} \neq 0$

- Introduce the quadratic flux $\varphi_2 \equiv \frac{1}{2} \iint d\vartheta \, d\zeta \left(\frac{\partial S}{\partial \vartheta} \right)^2$

- $\delta\varphi_2 = \iint d\vartheta \, d\zeta \; \delta\mathrm{P} \sqrt{g} \left(B^{\vartheta} \partial_{\vartheta} + B^{\zeta} \partial_{\zeta} \right) \bullet \upsilon$

$\upsilon \equiv \frac{\partial S}{\partial \vartheta} \equiv$ action-gradient

QFM surfaces are a family of extremal curves of the constrained-area action-integral

- $S \equiv \int_C \mathbf{A} \,.\, \mathbf{dl} - \upsilon \underbrace{\int_C (\vartheta \nabla\zeta .\mathbf{dl})}_{area=\int \vartheta(\zeta) d\zeta}$, where υ is a Lagrange multiplier
- Using an identity of vector calculus, $\delta S = \int_C \mathbf{dl} \times \left(\nabla \times \mathbf{A} - \upsilon \nabla\vartheta \times \nabla\zeta \right) \bullet \boldsymbol{\delta l}$
- extremal curves are tangential to the pseudo magnetic field

$\mathbf{B}_\upsilon \equiv \mathbf{B} - \upsilon \nabla\vartheta \times \nabla\zeta$

To find extremizing curves, use Newton method to set $\partial_\rho S=0$, $\partial_\vartheta S=0$

$\frac{\partial S}{\partial \rho_i} = 0$ reduces to $\frac{\partial S_i}{\partial \rho_i} = 0$, which can be solved locally, $\rho_i = \rho_i(\theta_{i-1}, \theta_i)$

$$\frac{\partial S}{\partial \theta_i} = \partial_2 S_i(\theta_{i-1}, \theta_i) + \partial_1 S_{i+1}(\theta_i, \theta_{i+1})$$

tridiagonal Hessian, inverted in O(N) operations, ***i.e. method is FAST***
This is "global" integration, and it is *not* required to follow magnetic field lines.

QFM surfaces ≡ family of periodic *pseudo* fieldlines, of the pseudo field $\mathbf{B}_\nu = \mathbf{B} - \nu\,\nabla\theta\times\nabla\zeta$

Usually, there are only the "stable" periodic fieldline and the "unstable" periodic fieldline,

$$\theta(\zeta + 2\pi q) = \theta(\zeta) + p\,2\pi/N$$

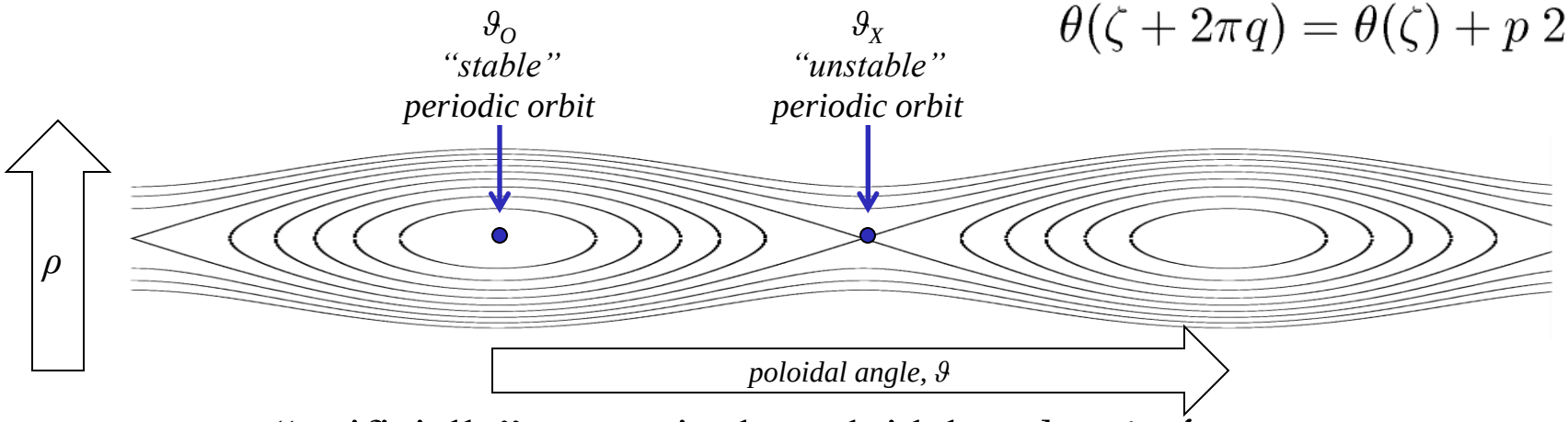

However, we can "artificially" constrain the poloidal angle, via $\int \theta\, d\zeta = const.$, and construct a family of periodic *pseudo* fieldlines that pass directly through the island

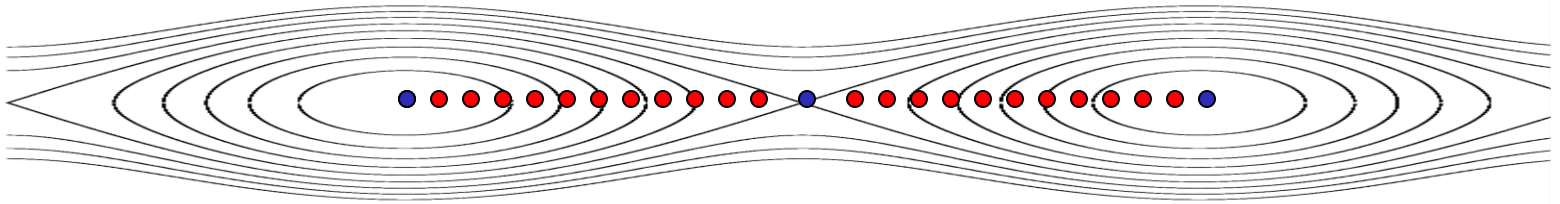

<u>A rational, quadratic-flux minimizing surface</u>
is a family of periodic, extremal curves of the constrained action integral, and
<u>is closely to related to the rational ghost-surface,</u>
which is defined by an action-gradient flow between the minimax periodic orbit and the minimizing orbit.

$$\varphi_2 \equiv \tfrac{1}{2}\int_\Gamma w|B_n|^2\,dS,$$

The "upward" flux = "downward" flux across a toroidal surface passing through an island chain can be computed.

$$\int_{\partial\mathcal{V}} \mathbf{B}\cdot d\mathbf{S} \equiv \int_{\mathcal{V}} \nabla\cdot\mathbf{B} = 0$$

the total flux across any closed surface of a divergence free field is zero.

$$\int_{\mathcal{S}} \mathbf{B}\cdot d\mathbf{s} \equiv \int_{\partial\mathcal{S}} \mathbf{A}\cdot d\mathbf{l} \qquad \Psi_{p/q} \equiv \int_{O} \mathbf{A}\cdot d\mathbf{l} - \int_{X} \mathbf{A}\cdot d\mathbf{l}$$

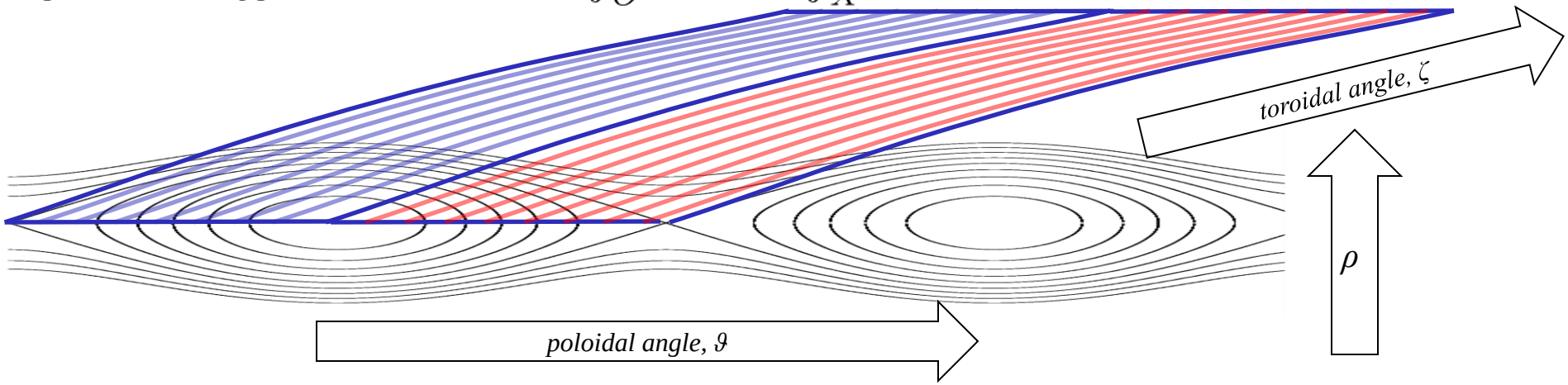

consider a sequence of rationals, *p/q*, that approach an irrational, ι

$$\text{If } \Psi_{p/q} \to 0 \text{ as } p/q \to \iota, \text{ then KAM surface exists}$$

If $\Psi_{p/q} \to \Delta$, where $\Delta \neq 0$, then the KAM surface is "broken", and $\Psi_{p/q}$ is the upward-flux across the cantorus

The field near the edge of LHD is chaotic, because of the overlap of low-order islands.

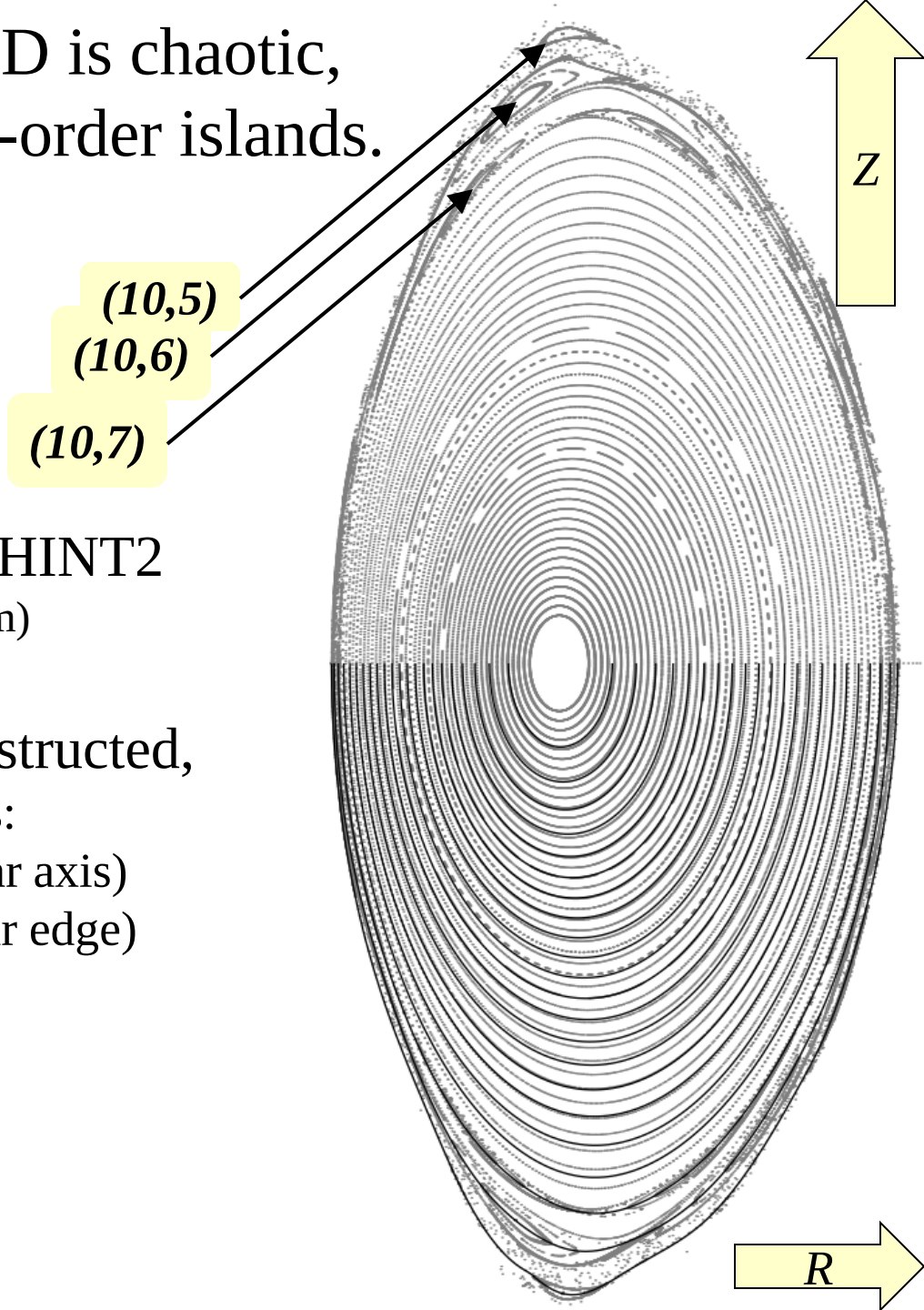

The magnetic field is provided by HINT2
(but this calculation is for the standard vacuum)

A selection of QFM surfaces is constructed,
shown with black lines, with periodicities:

(10,23), (10,22), (10,21), . . . (near axis)
. . . , (10,9), (10,8), (10,7), (10,6), (near edge)

For non-integrable fields, field line transport is restricted by KAM surfaces and cantori

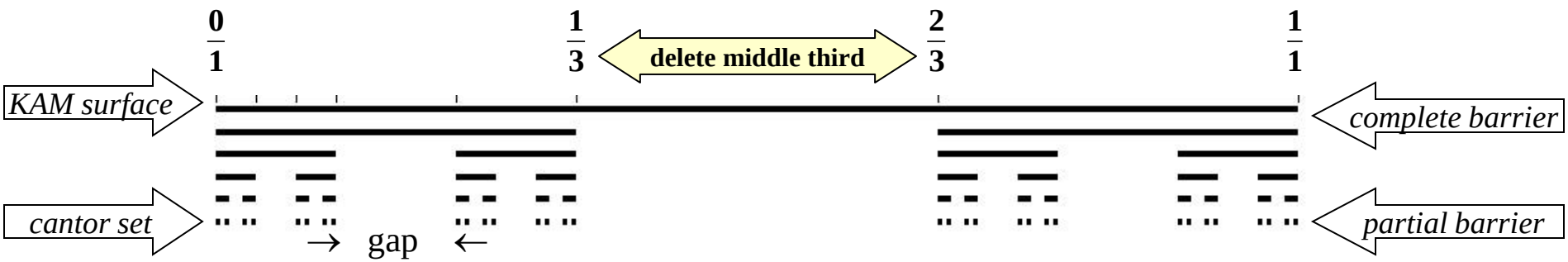

→ KAM surfaces are closed, toroidal surfaces that **stop** radial field line transport

→ Cantori have "gaps" that fieldlines can pass through; however, **cantori can severely restrict** radial transport

→ Example: all flux surfaces destroyed by chaos, but even after **100 000 transits** around torus the fieldlines **cannot get past cantori**

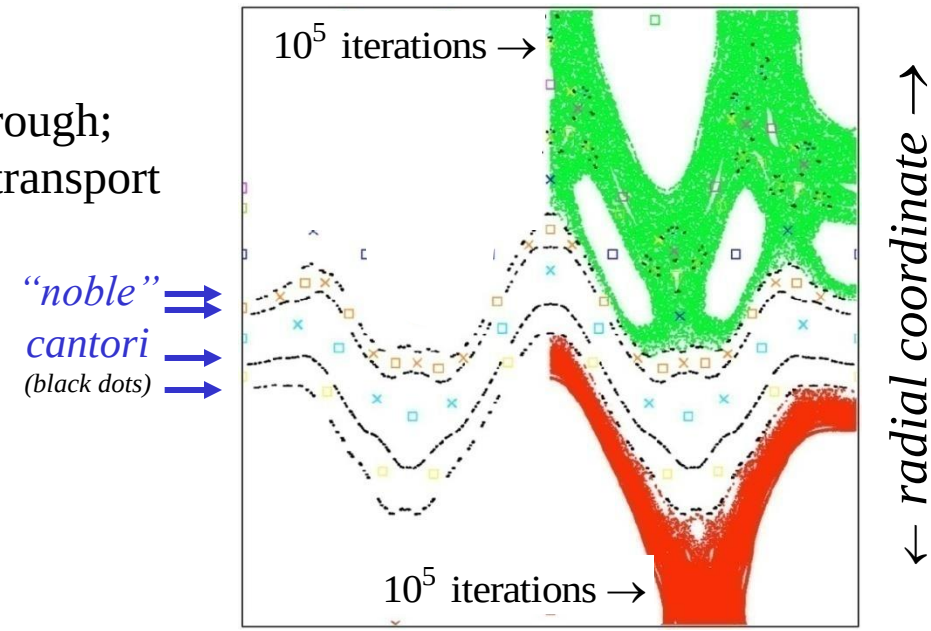

The fractal structure of chaos is related to the structure of rationals and irrationals on the number line.

Farey Tree

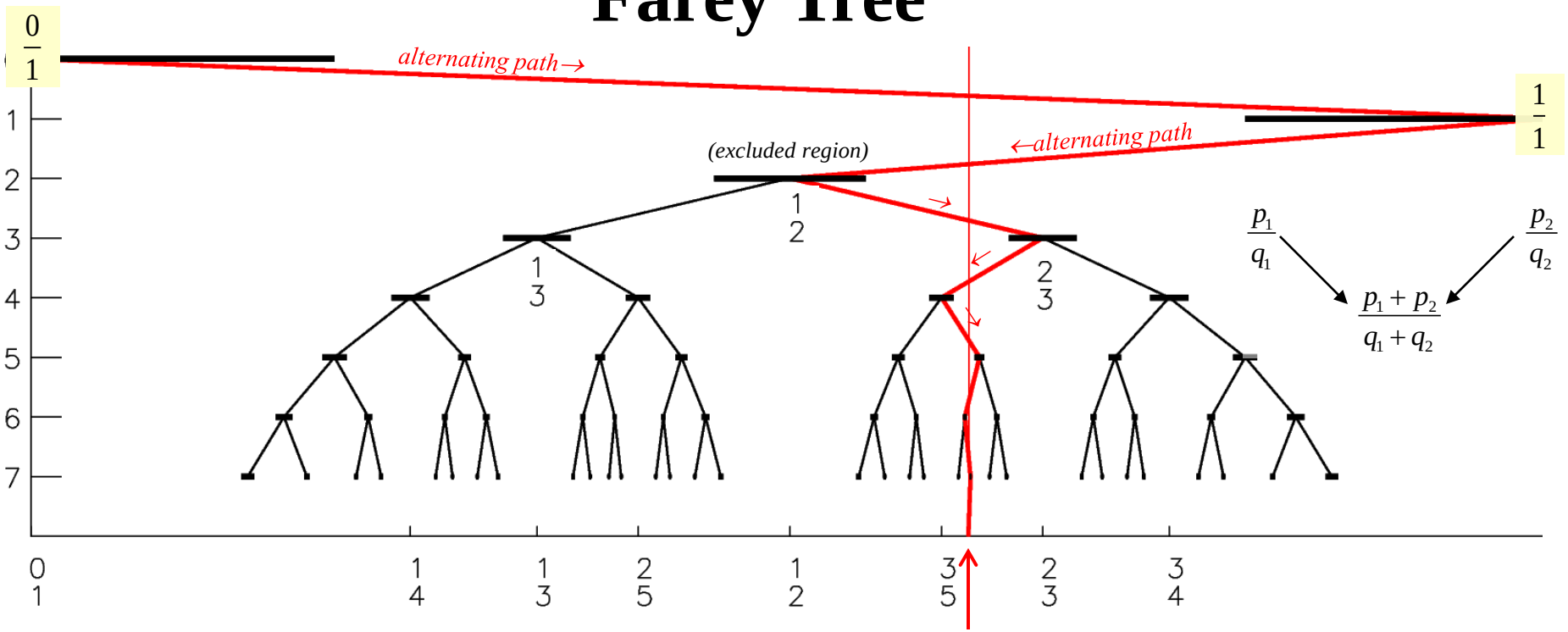

islands & chaos emerge at every rational → about each rational n/m, introduce excluded region, width r/m^k

KAM Theorem → flux surface can survive if $|\omega - n/m| > r/m^k$, for all n, m

(Kolmogorov, Arnold, Moser) *we say that ω is "strongly-irrational" if ω avoids all excluded regions*

Greene's residue criterion → the most robust flux surfaces are associated with alternating paths

→ Fibonacci ratios $\frac{0}{1}, \frac{1}{1}, \frac{1}{2}, \frac{2}{3}, \frac{3}{5}, \frac{5}{8}, \frac{8}{13}, \frac{13}{21}, \frac{21}{34}, \ldots$

Using these low-order QFM surfaces as coordinate surfaces, the low-order islands become straight.

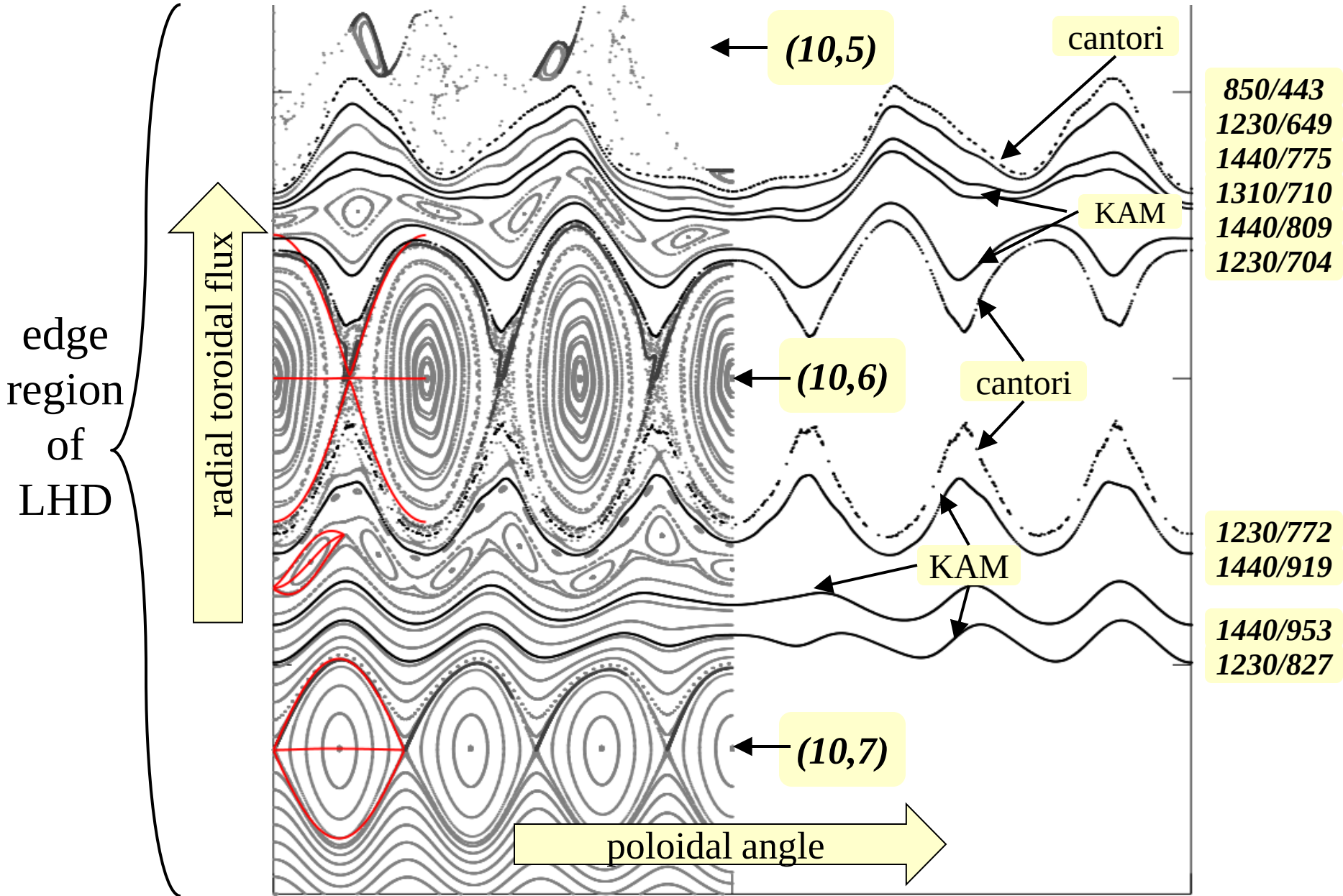

The Flux Farey tree shows the flux across the rational surfaces.

- The flux across a rational surface is $\Psi_{p/q} \equiv \int_O \mathbf{A} \cdot d\mathbf{l} - \int_X \mathbf{A} \cdot d\mathbf{l}$
- The "more irrational" the periodicity, the lower the flux.
- If $\Psi_{p/q} \to 0$ as $q \to \infty$, a KAM surface exists.
- Otherwise, the limiting $\Psi_{p/q}$ is the flux across the cantorus;

  this indicates the importance of that cantorus as a *partial* barrier.

Flux Farey Tree

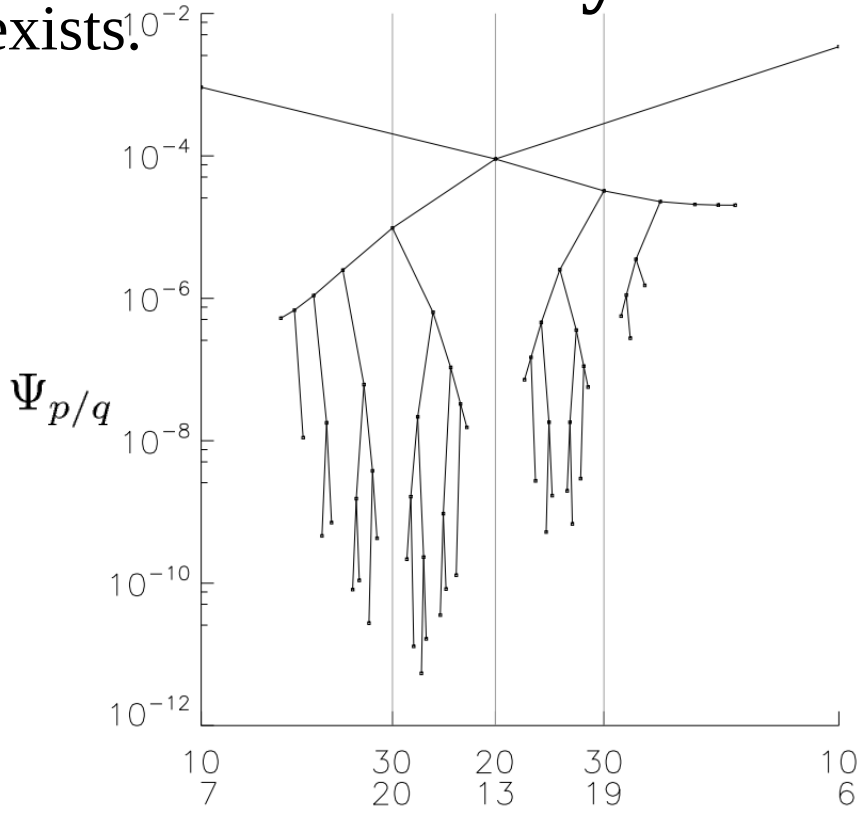

Greene's residue criterion determines the existence of irrational surfaces, including the last-closed flux surface.

- The residue quantifies the "stability" of a periodic orbit
  $R_{p/q} = (2-\lambda-1/\lambda)/4$, where λ is eigenvalue of tangent map

Consider a sequence (p_i,q_i) s.t. $p/q \rightarrow \iota$, where ι is irrational

- If $R_{p/q} \rightarrow 0$,
  the surface exists
- If $R_{p/q} \rightarrow 0.25$,
  the surface is critical
- If $R_{p/q} \rightarrow \infty$,
  the surface is destroyed

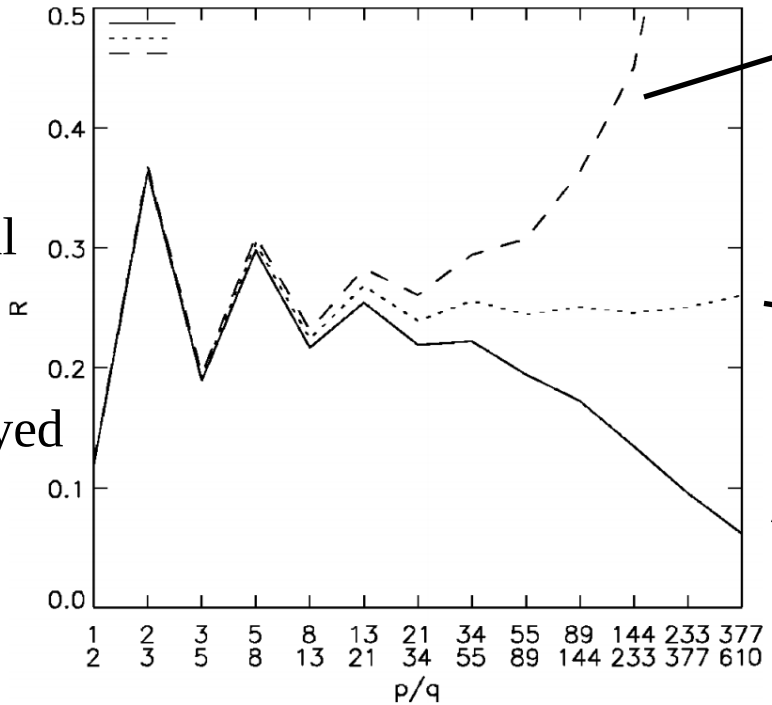

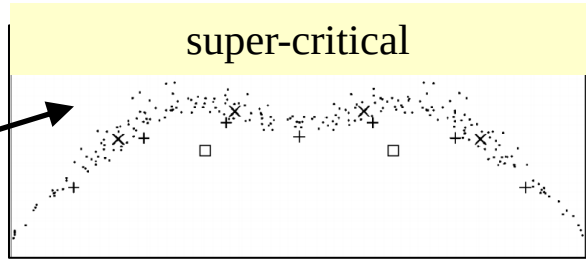

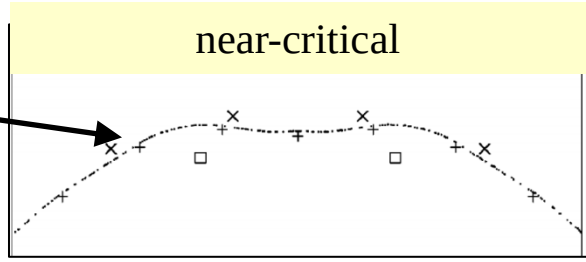

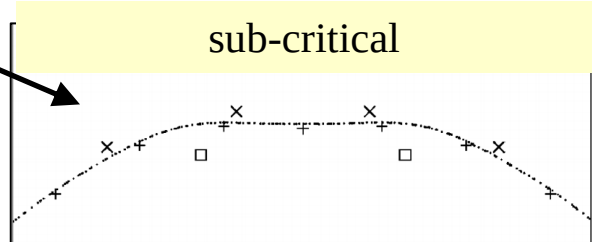

Now, back to the edge of LHD;
construct a set of high-order QFM surfaces,

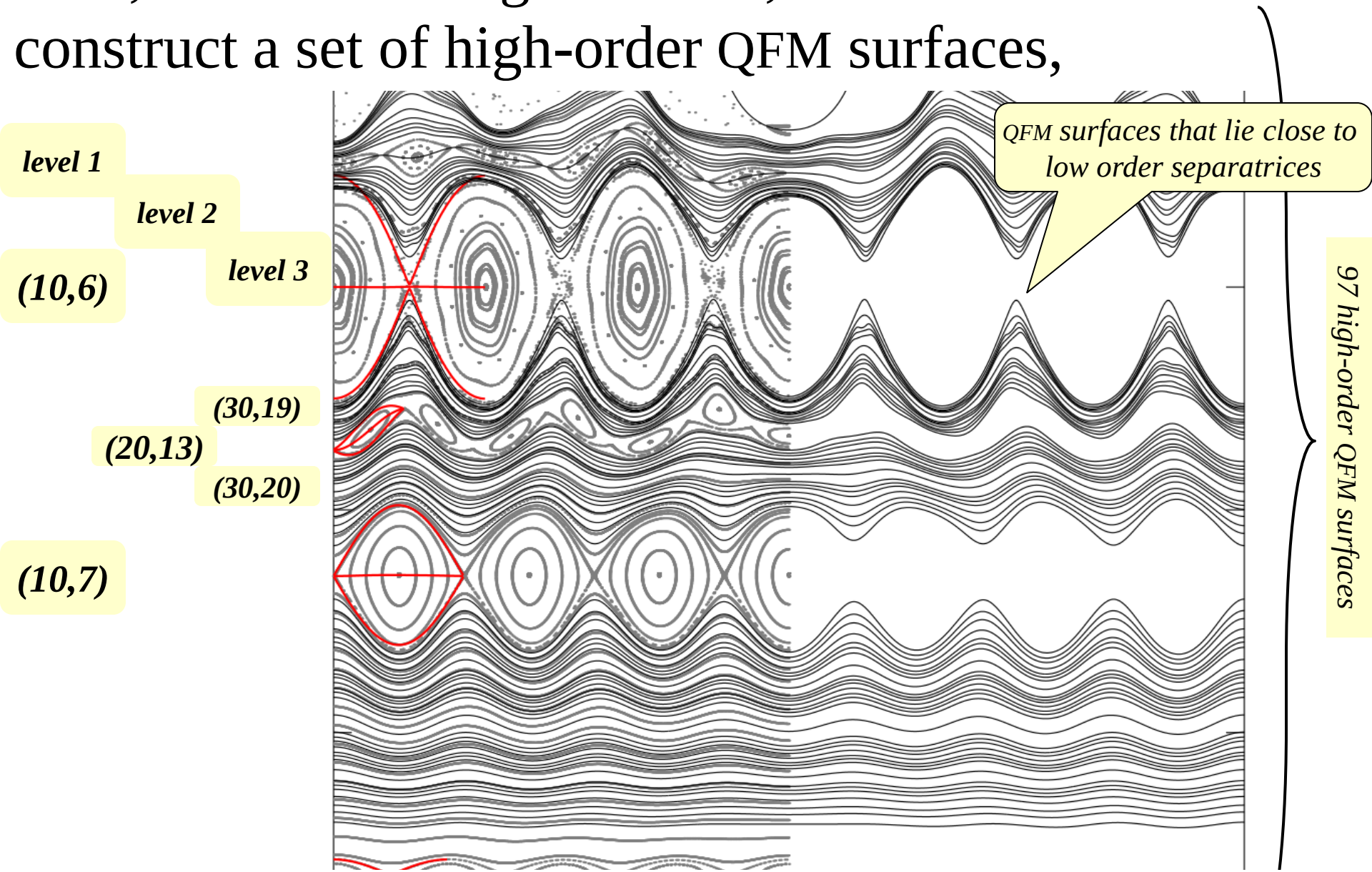

and use these surfaces as coordinate surfaces . . .

In *chaotic-coordinates*™, the flux surfaces are straight, and the islands are square.

These coordinates can simplify many calculations, e.g.

pressure = p(s)

temperature = T(s)

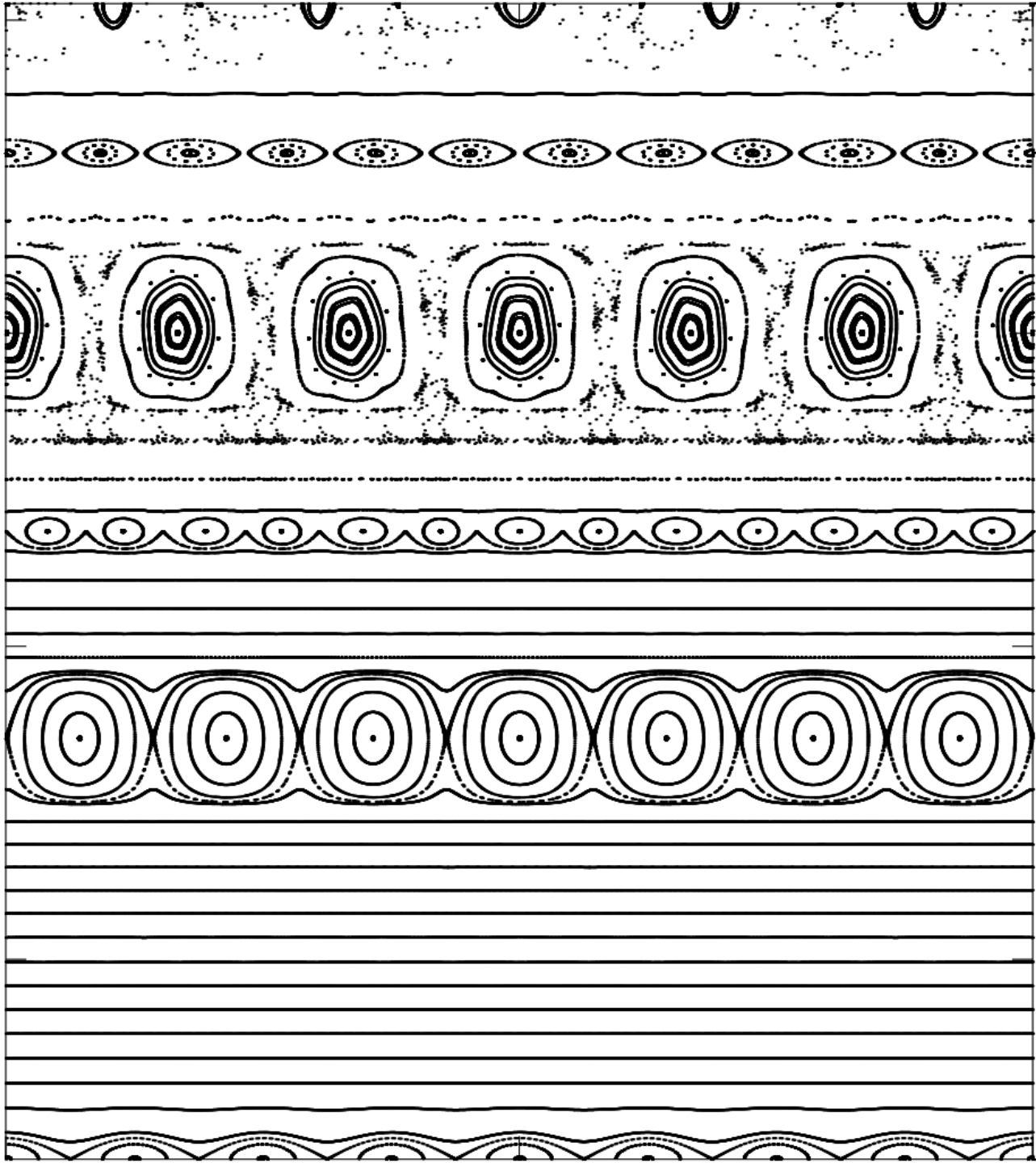

Chaotic coordinates simplify anisotropic transport: the temperature is constant on ghost surfaces, $T=T(s)$

1. Transport <u>along</u> the magnetic field is <u>unrestricted</u>
→ consider parallel random walk, with **<u>long</u>** steps≈ collisional mean free path

2. Transport <u>across</u> the magnetic field is <u>very small</u>
→consider perpendicular random walk with **<u>short</u>** steps≈ Larmor radius

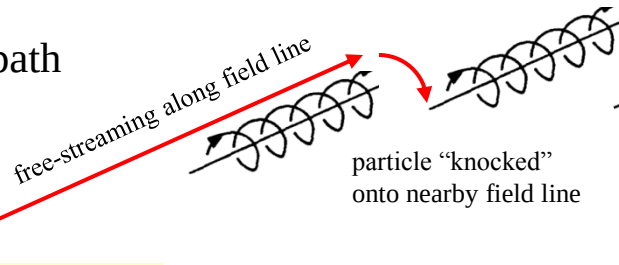

3. Anisotropic diffusion balance $\kappa_{\|}\,\nabla_{\|}^2\,T+\kappa_{\perp}\,\nabla_{\perp}^2\,T=0\,,\quad \kappa_{\|}\gg\kappa_{\perp},\quad \kappa_{\perp}\big/\kappa_{\|}\sim 10^{-10}$

$2^{12}\times 2^{12} = 4096\times 4096$ grid points
(to resolve small structures)

4. Compare solution of numerical calculation to ghost-surfaces

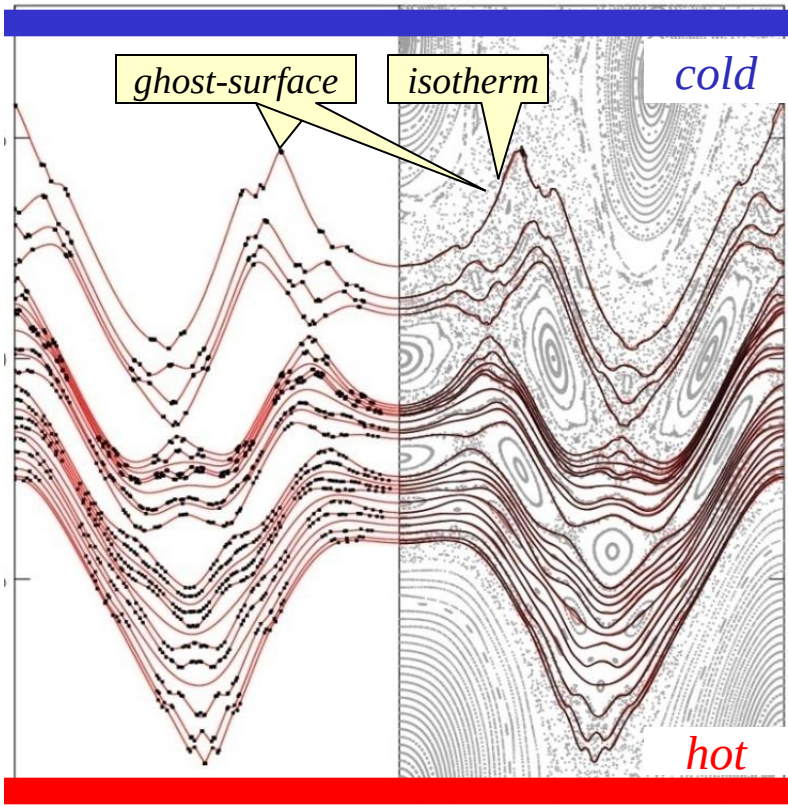

5. The temperature adapts to KAM surfaces, cantori,
and ghost-surfaces!
i.e. T=T(s), where s=const. is a ghost-surface

6. From T=T(s,θ,ϕ) to T=T(s) is a fantastic simplification, allows analytic solution

$$\frac{d\,T}{d\,s}\propto\frac{1}{\kappa_{\|}\,\varphi_2\,+\,\kappa_{\perp}\,G}$$

7. A long term goal of this effort into constructing chaotic coordinates is to determine if the pressure relaxation algorithm in HINT2 can be replaced.

To illustrate, we examine the standard configuration of LHD

The initial coordinates are axisymmetric, circular cross section,

$R = 3.63 + \rho\ 0.9 \cos\vartheta$

$Z = \quad\ \rho\ 0.9 \sin\vartheta$ which are *not* a good approximation to flux coordinates!

Poincaré plot in cylindrical coordinates

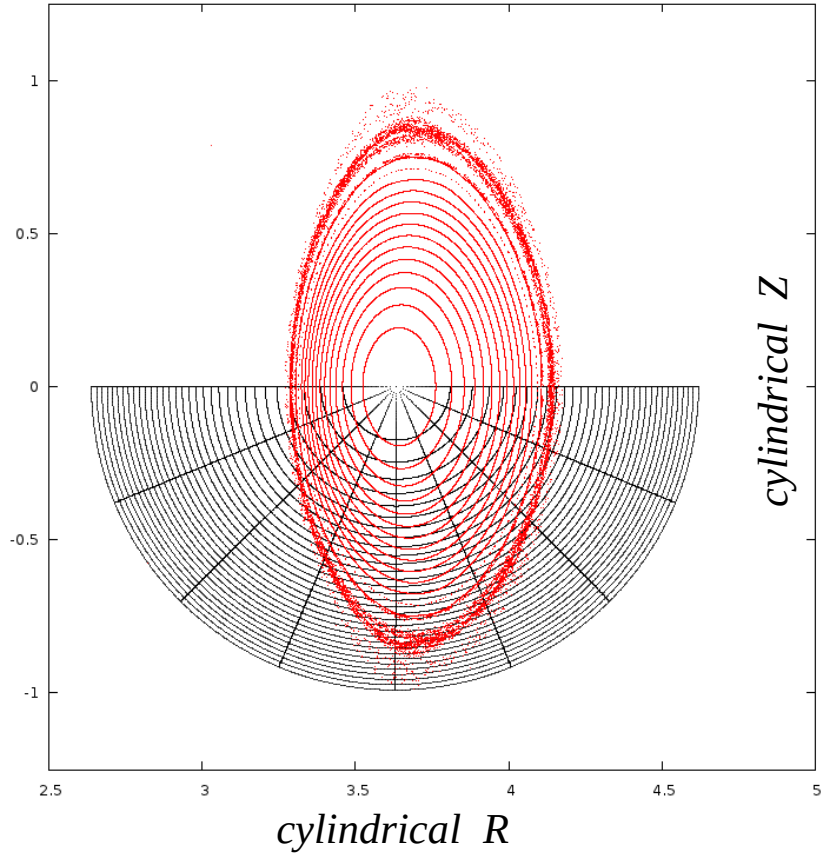

Poincaré plot in toroidal coordinates

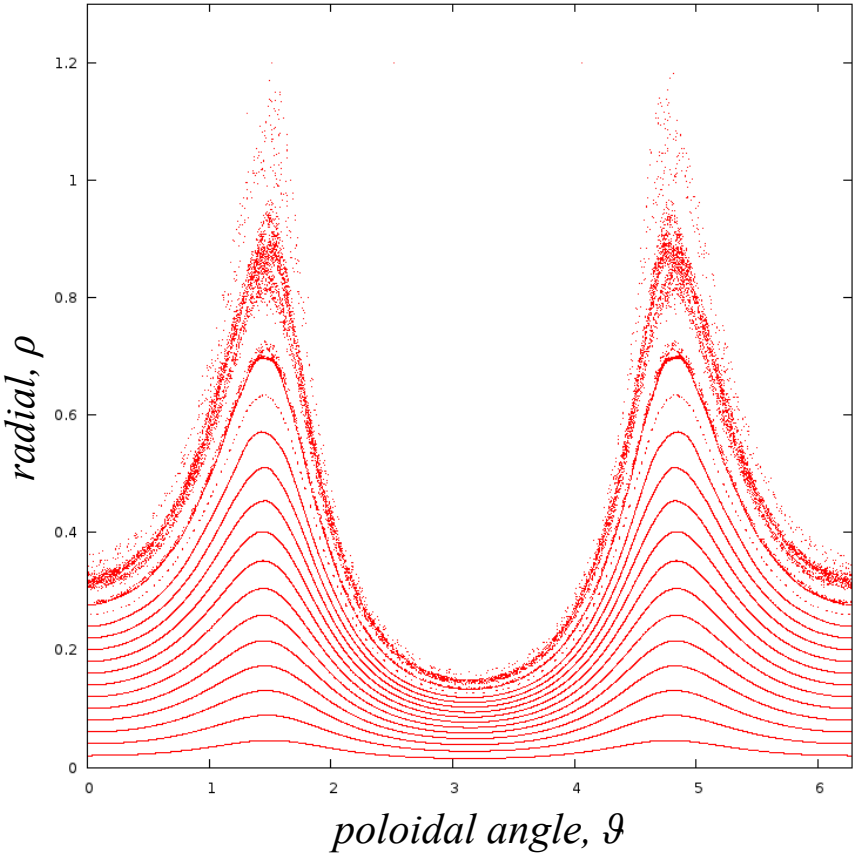

We construct coordinates that *better* approximate straight-field line flux coordinates,

by constructing a set of rational, almost-invariant surfaces, e.g. the (1,1), (1,2) surfaces

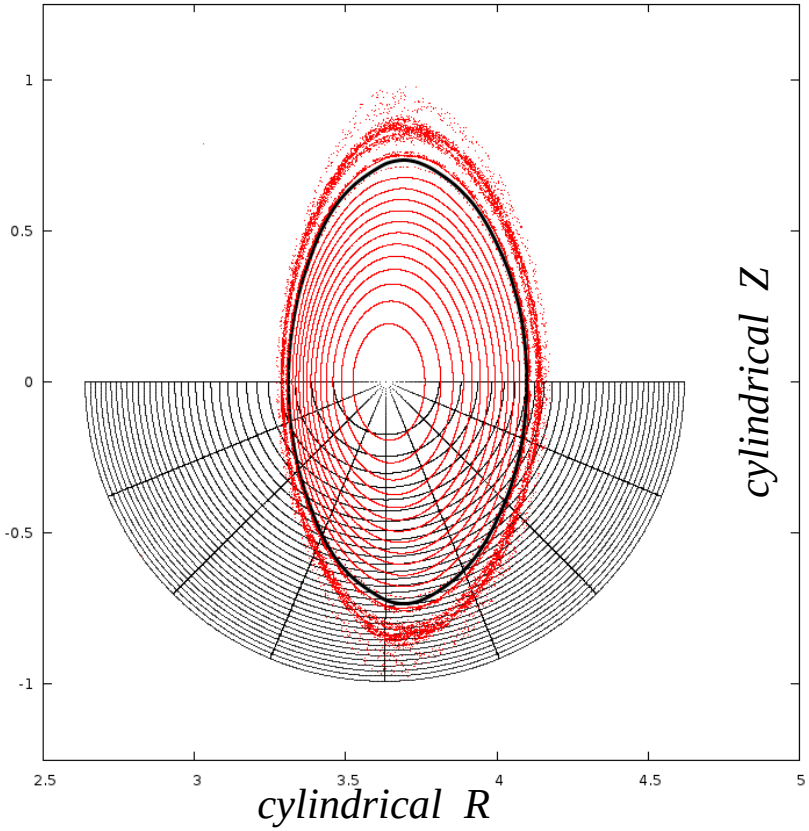

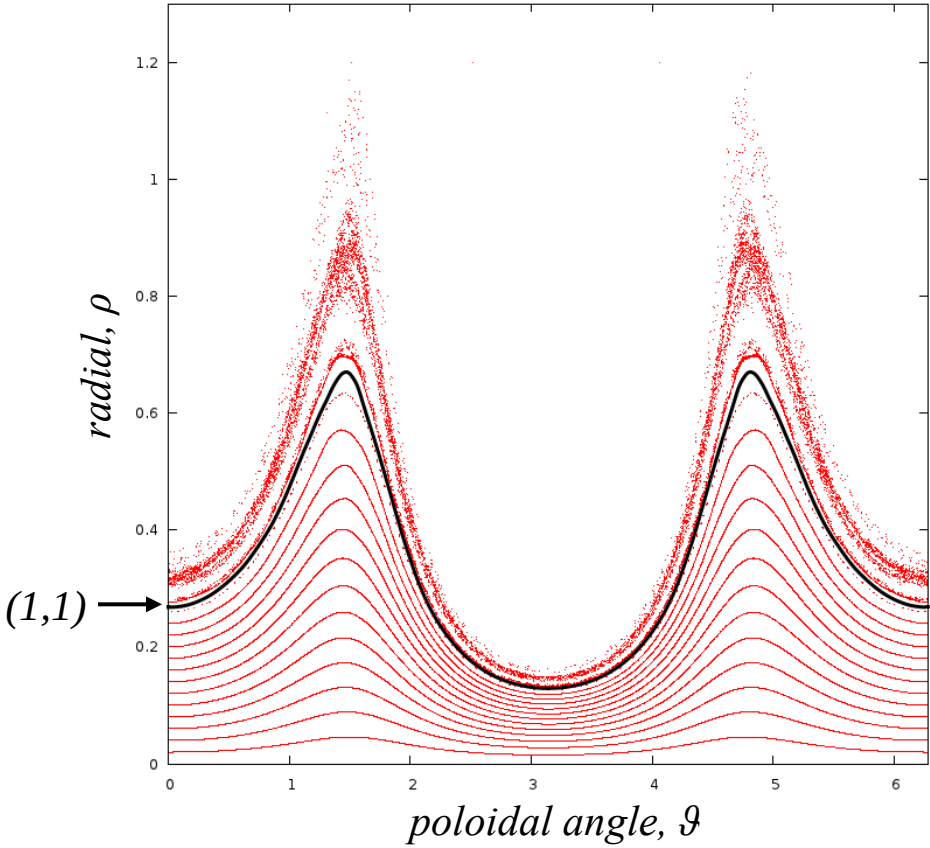

838 / 841

A Fourier representation of the (1,1) rational surface is constructed,

$R = R(\alpha,\zeta) = \sum R_{m,n} \cos(m\,\alpha - n\,\zeta)$

$Z = Z(\alpha,\zeta) = \sum Z_{m,n} \sin(m\,\alpha - n\,\zeta)$,

where α is a straight field line angle

Updated coordinates:
the (1,1) surface is used as a coordinate surface.

The updated coordinates are a better approximation to straight-field line flux coordinates, and the flux surfaces are (almost) flat

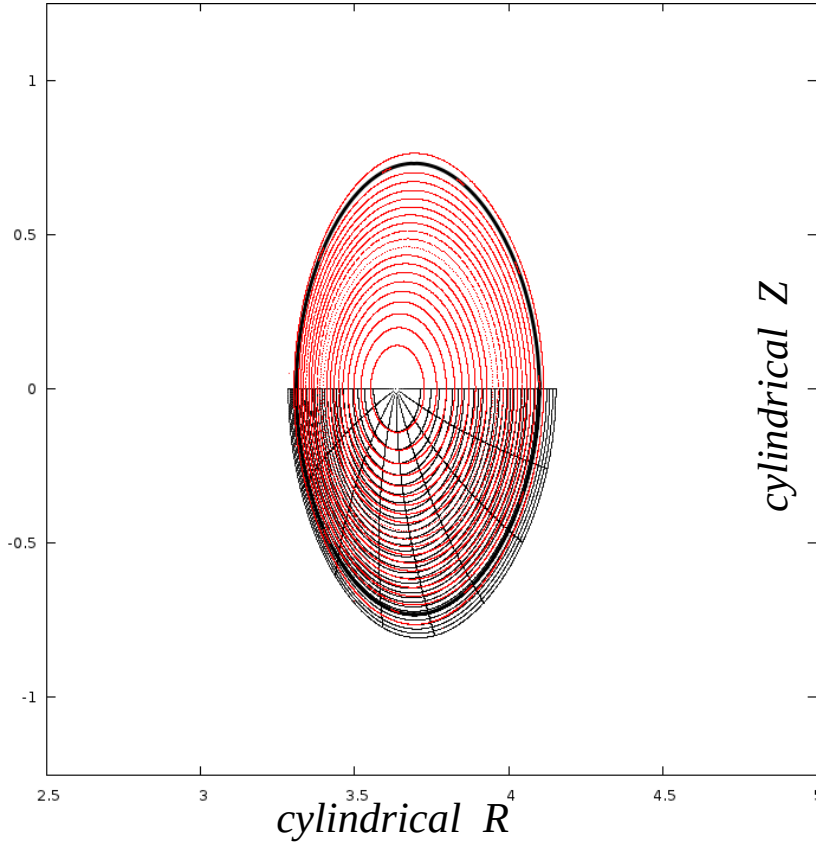

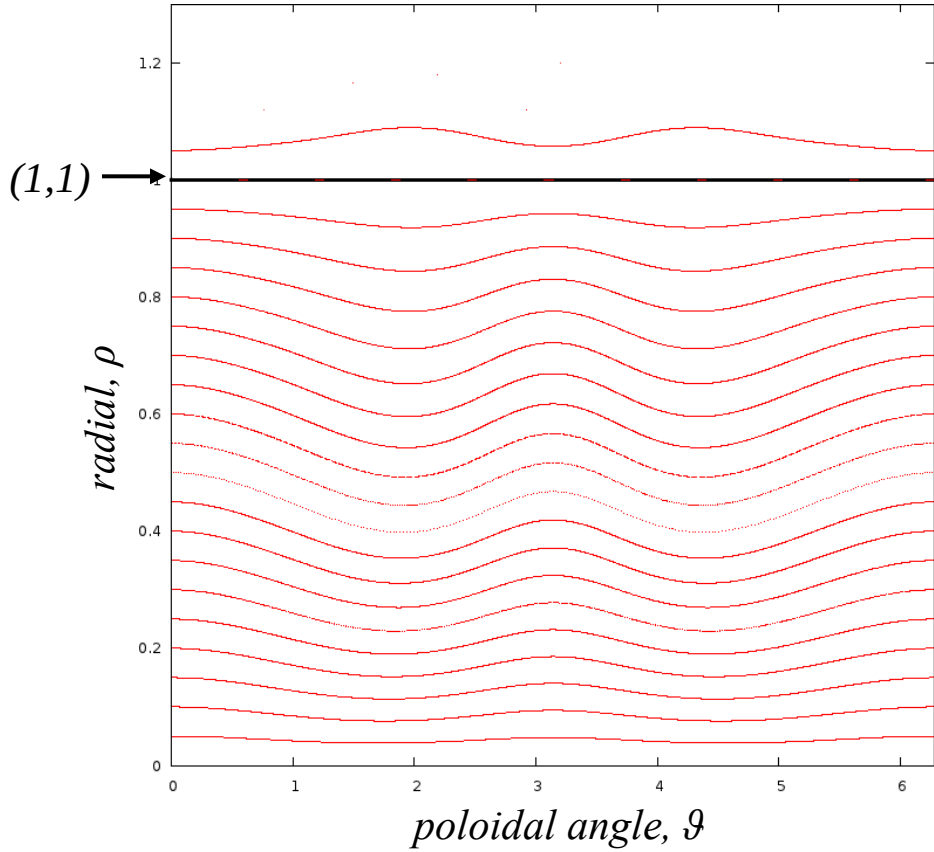

Now include the (1,2) rational surface

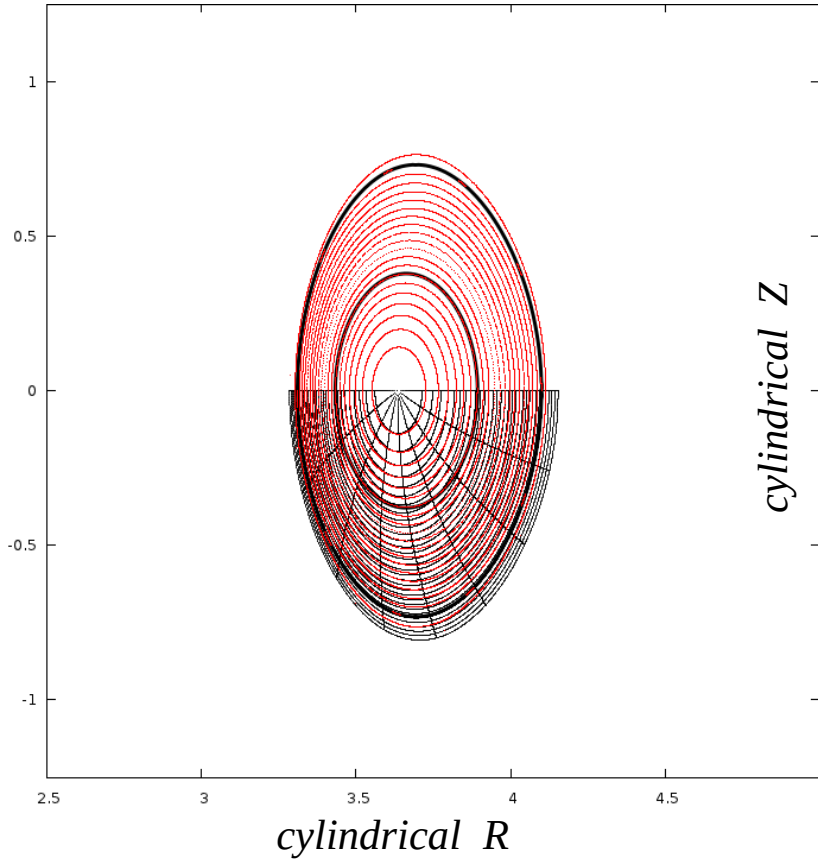

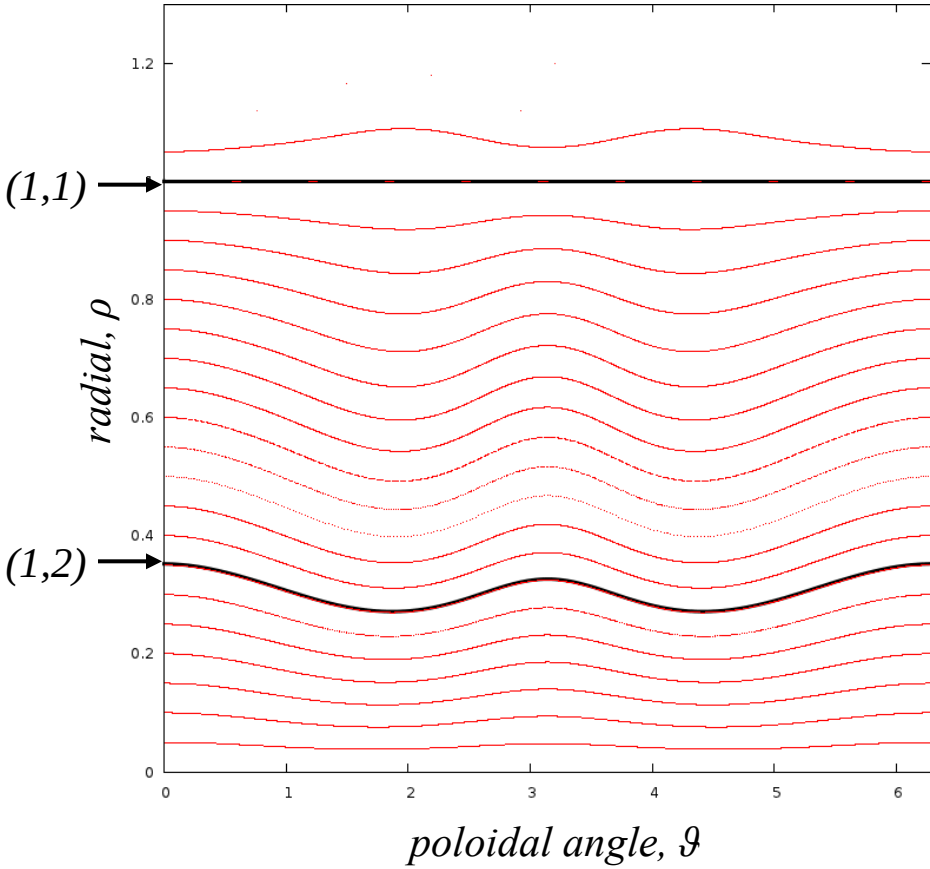

Updated coordinates:
the (1,1) surface is used as a coordinate surface
the (1,2) surface is used as a coordinate surface

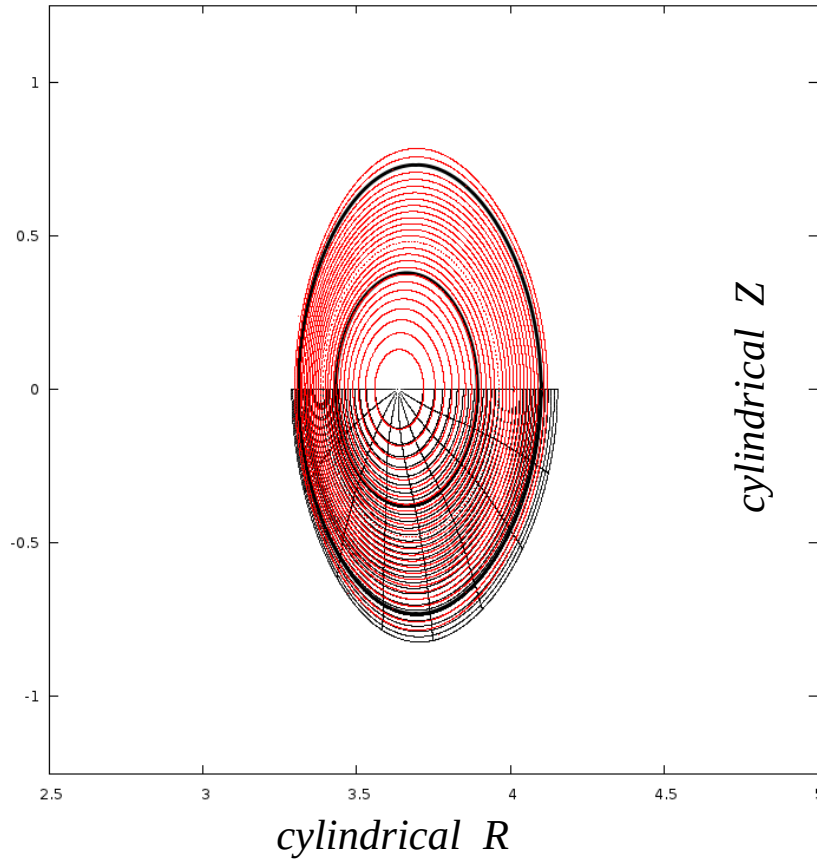

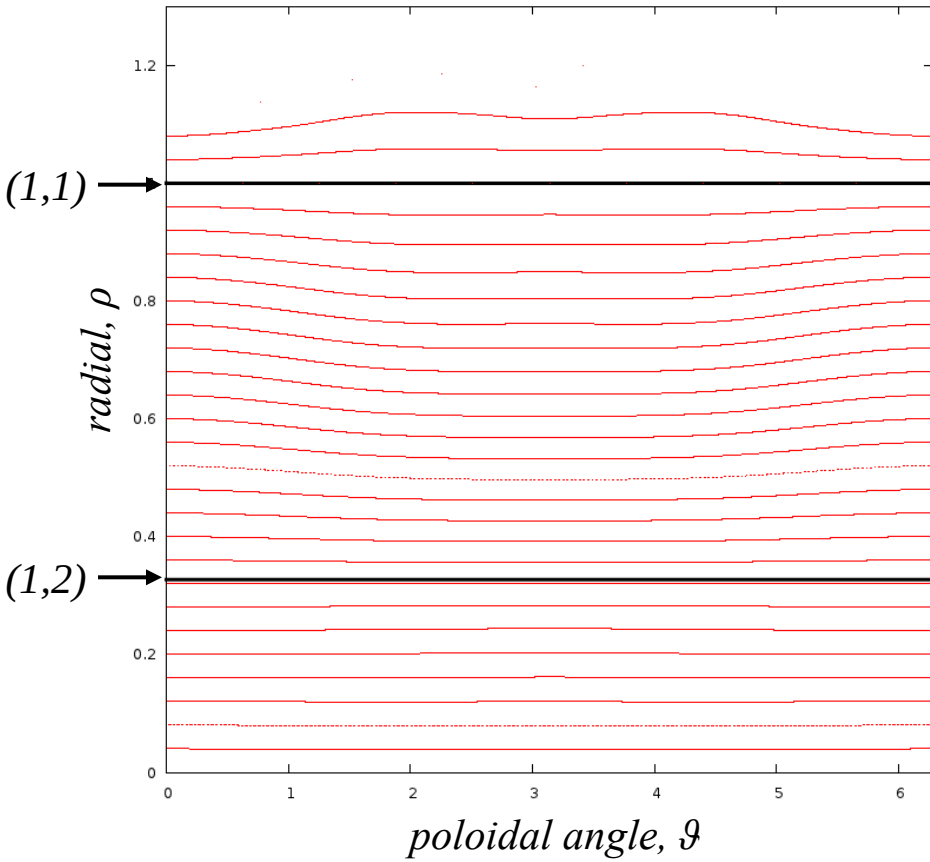

Now include the (2,3) rational surface

Note that the (1,1) and (1,2) surfaces have previously been constructed and are used as coordinate surfaces, and so these surfaces are flat.

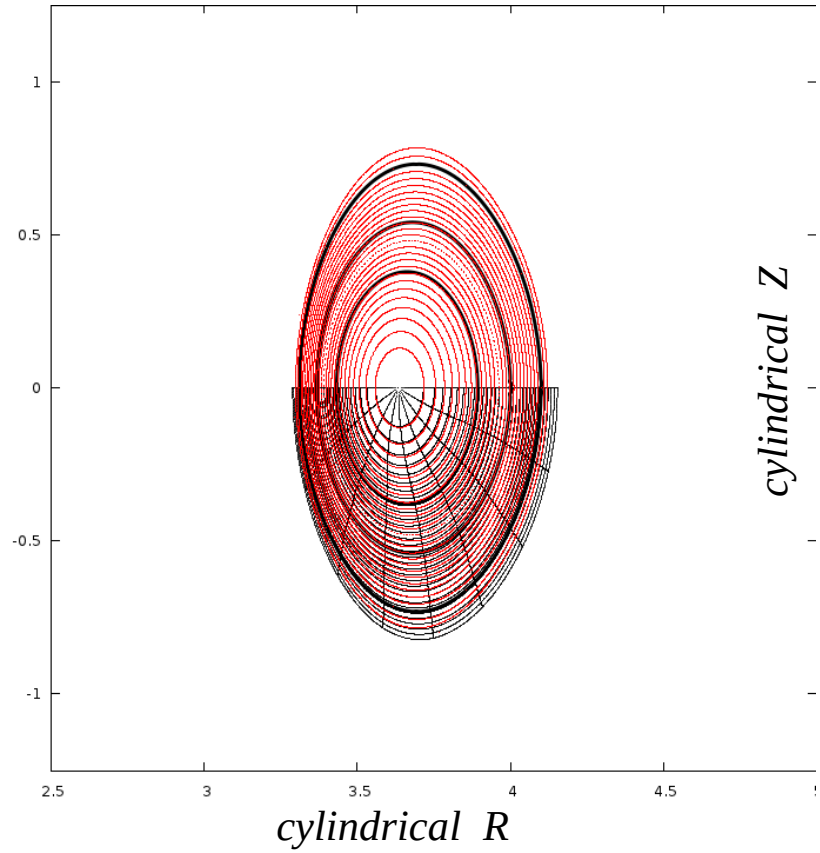

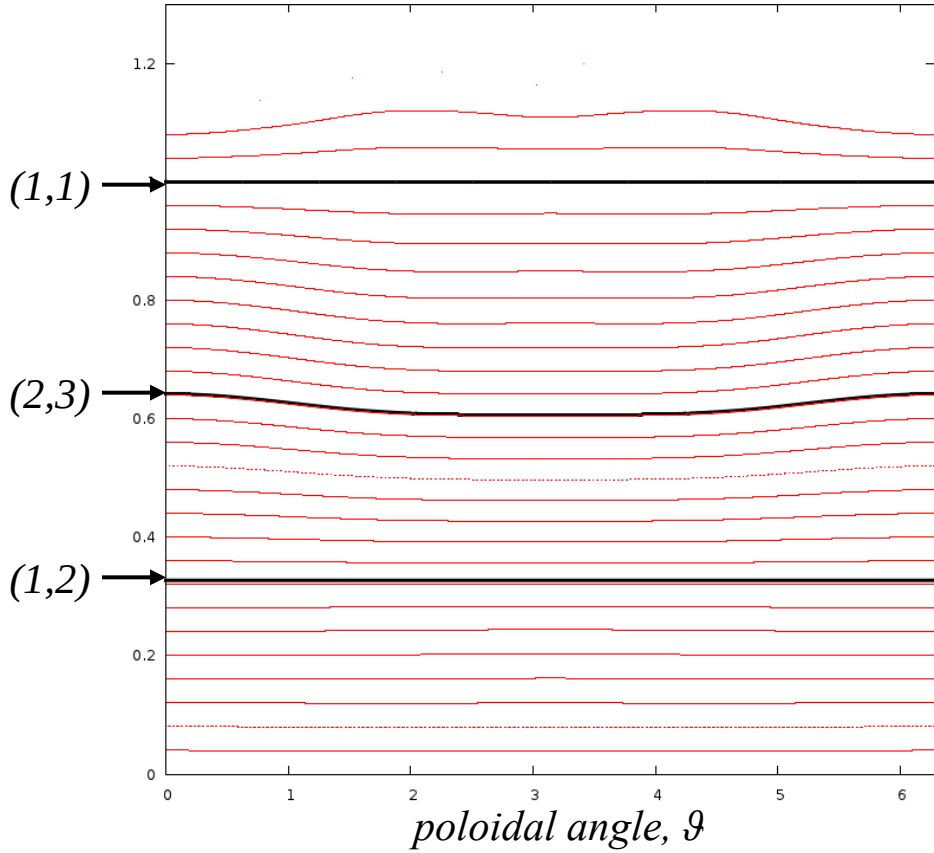

Updated Coordinates:

the (1,1), (2,3) & (1,2) surfaces are used as coordinate surfaces

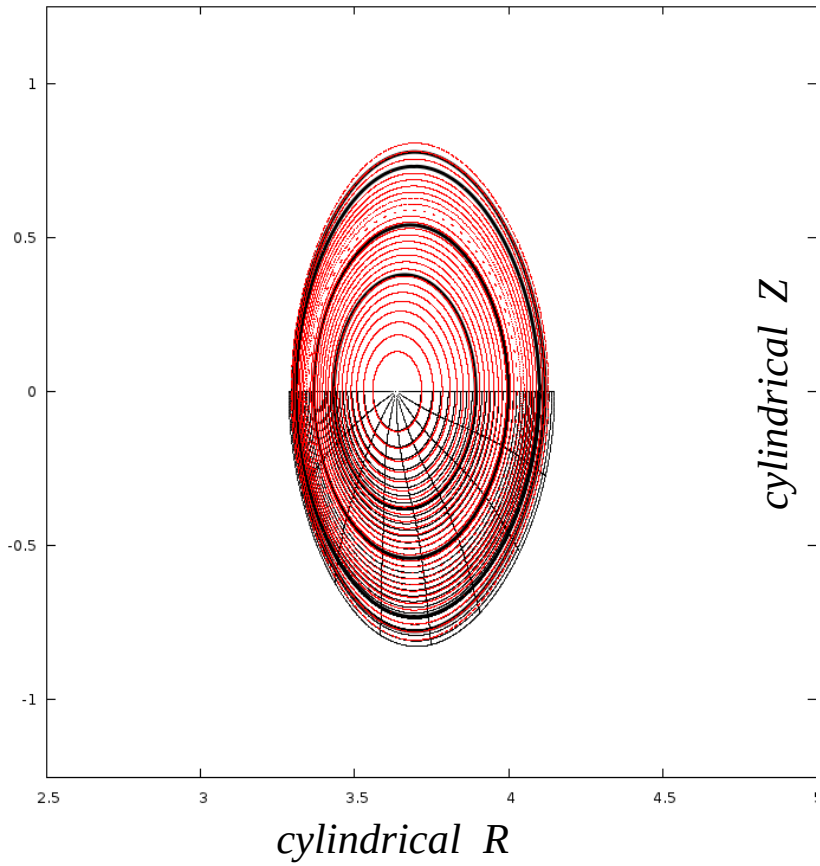

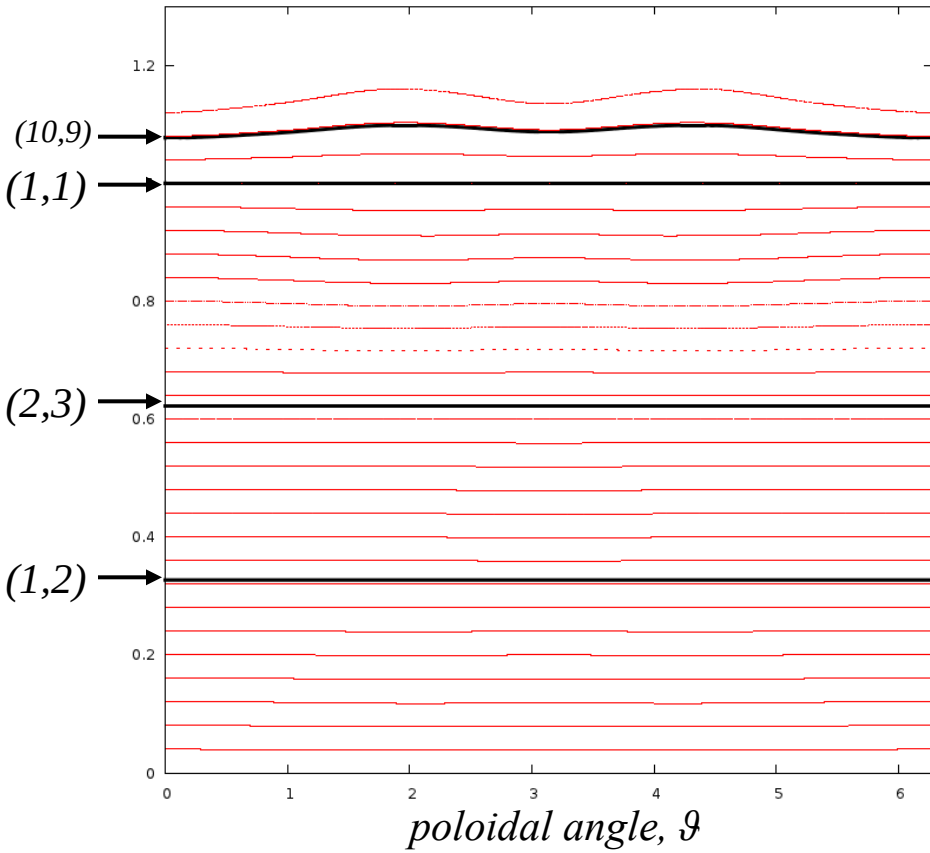

New Coordinates, the (10,9) surface is used as the coordinate boundary
the (1,1) surface is used as a coordinate surface
the (2,3) surface is used as a coordinate surface
the (1,2) surface is used as a coordinate surface

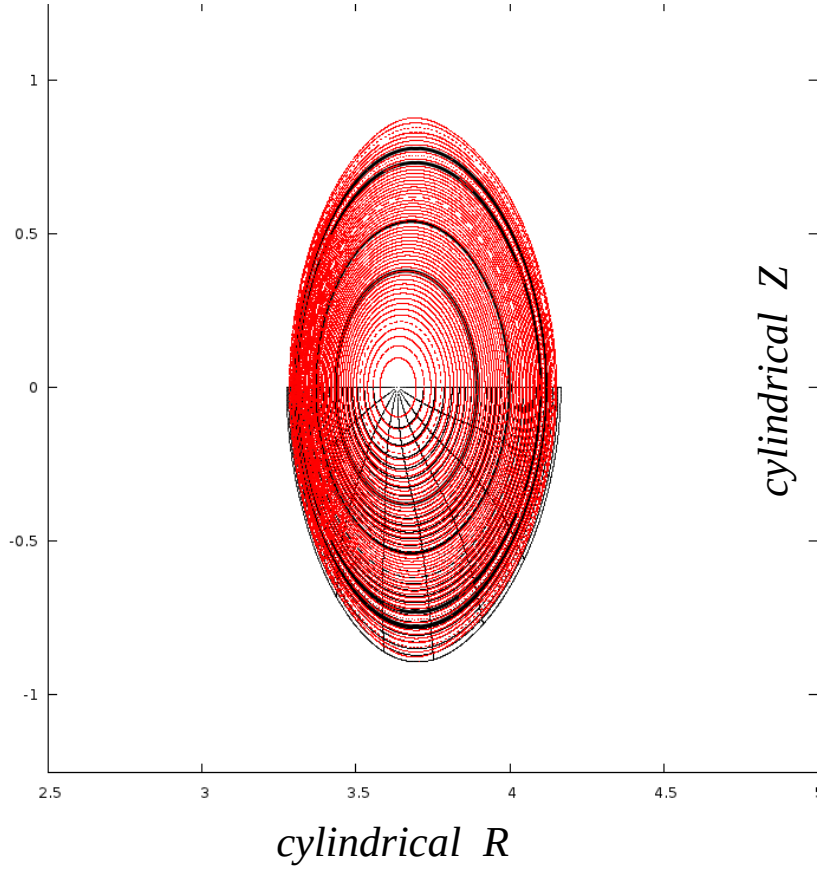

Poincare plot

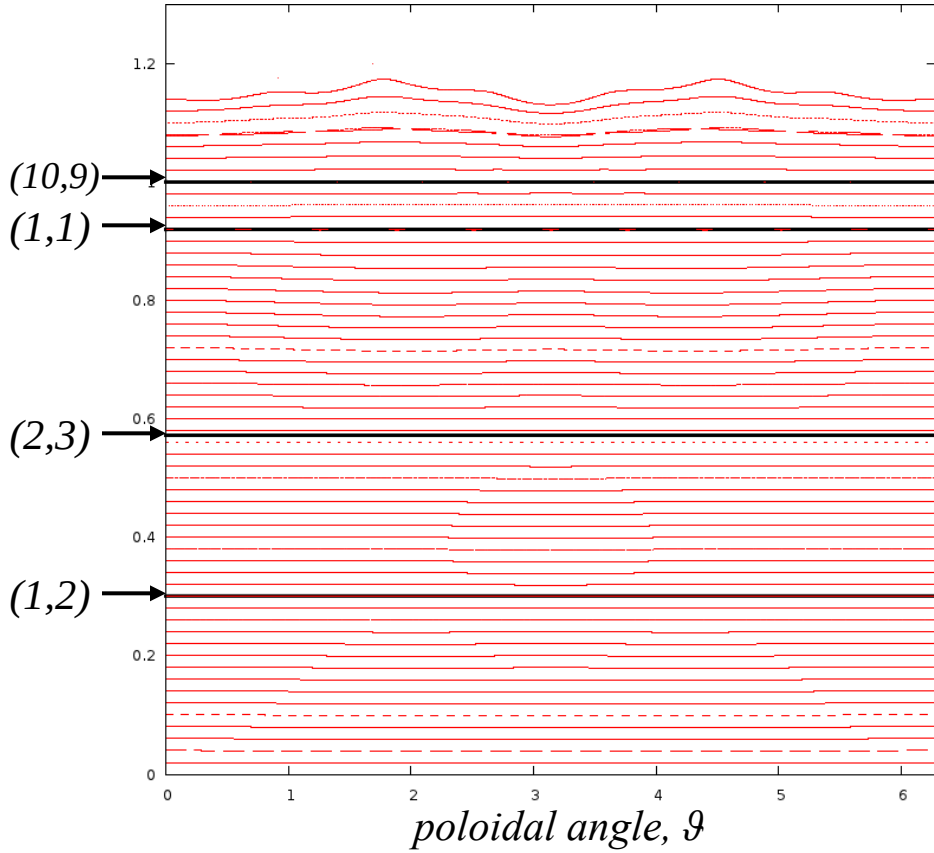

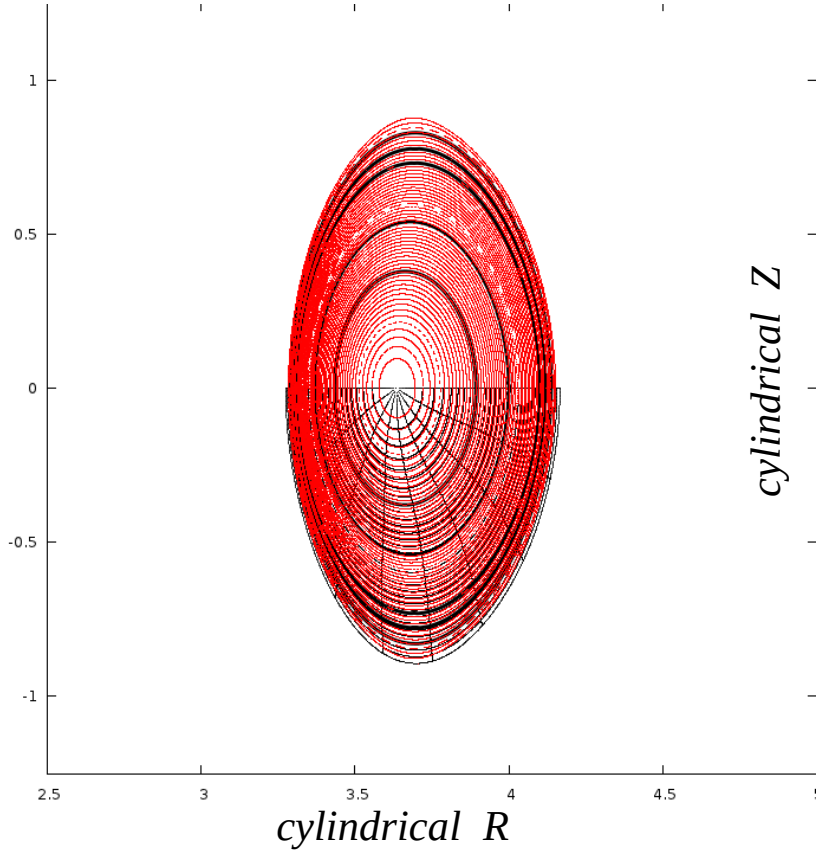
1
0.5
0
-0.5
-1
2.5
3
3.5
4
4.5
cylindrical R
cylindrical Z

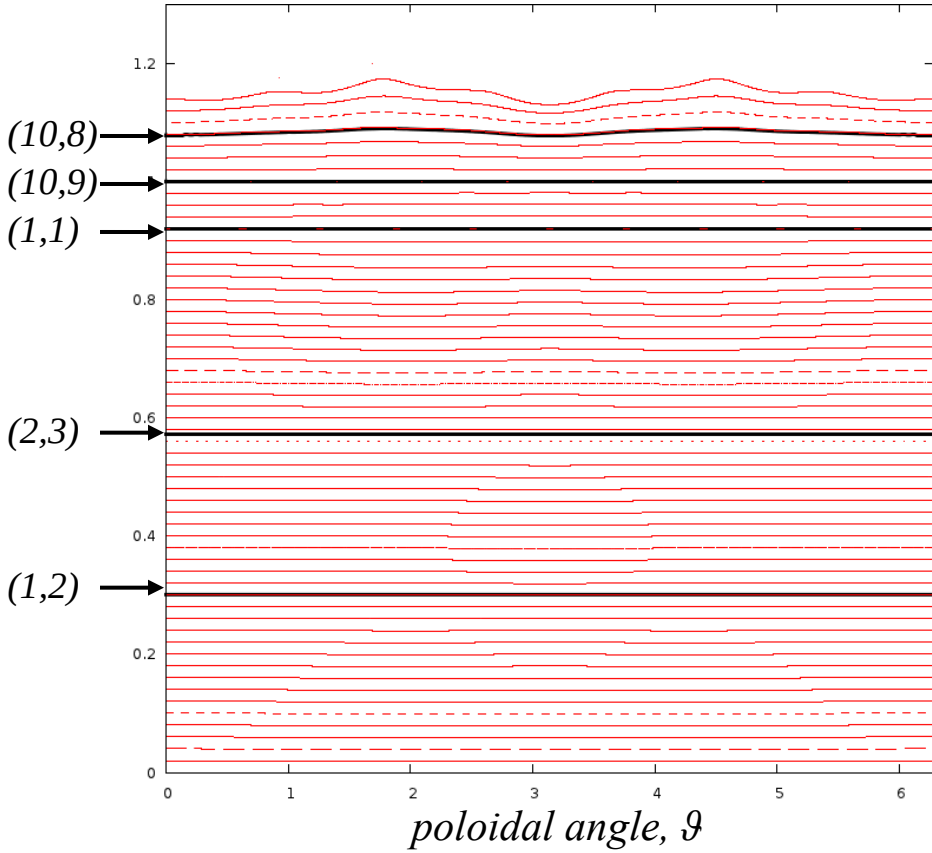
(10,8)
(10,9)
(1,1)
(2,3)
(1,2)
1.2
0.8
0.6
0.4
0.2
0
0
1
2
3
4
5
6
poloidal angle, ϑ

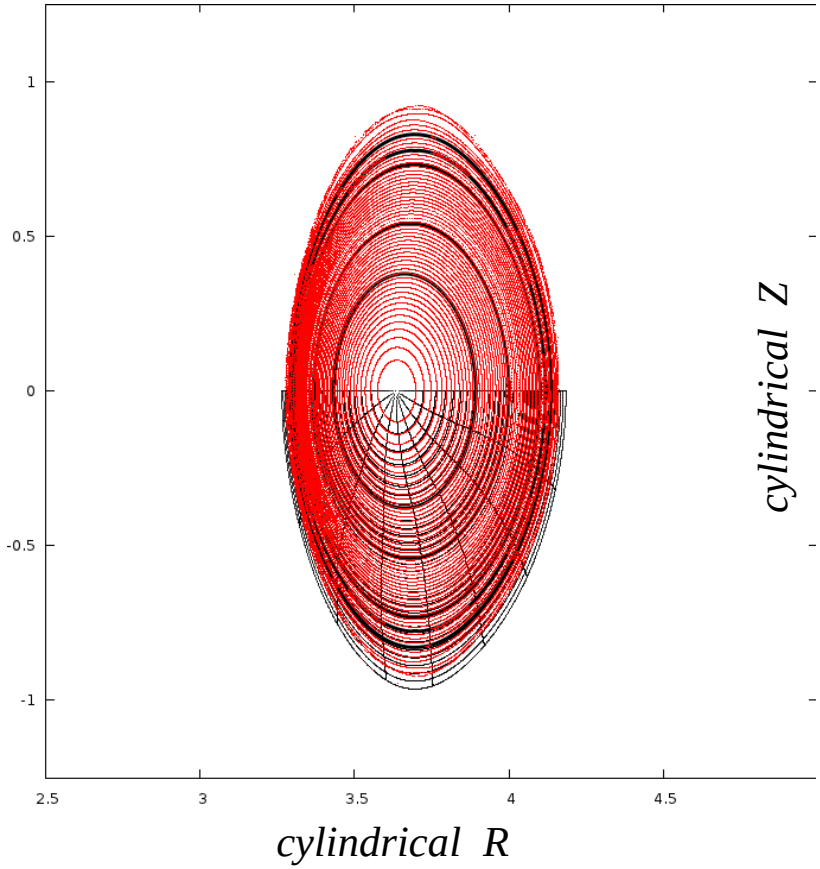
1
0.5
0
-0.5
-1
2.5
3
3.5
4
4.5
cylindrical R
cylindrical Z

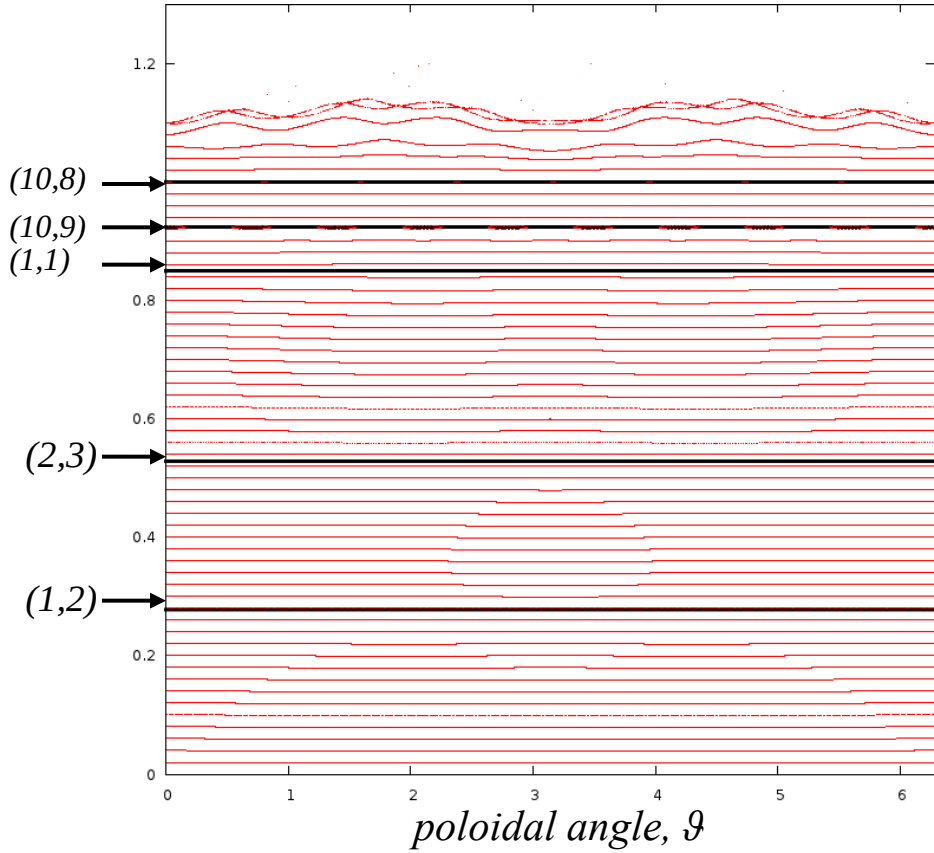
(10,8)
(10,9)
(1,1)
(2,3)
(1,2)
1.2
0.8
0.6
0.4
0.2
0
0
1
2
3
4
5
6
poloidal angle, ϑ

Straight field line coordinates can be constructed over the domain where invariant flux surfaces exist

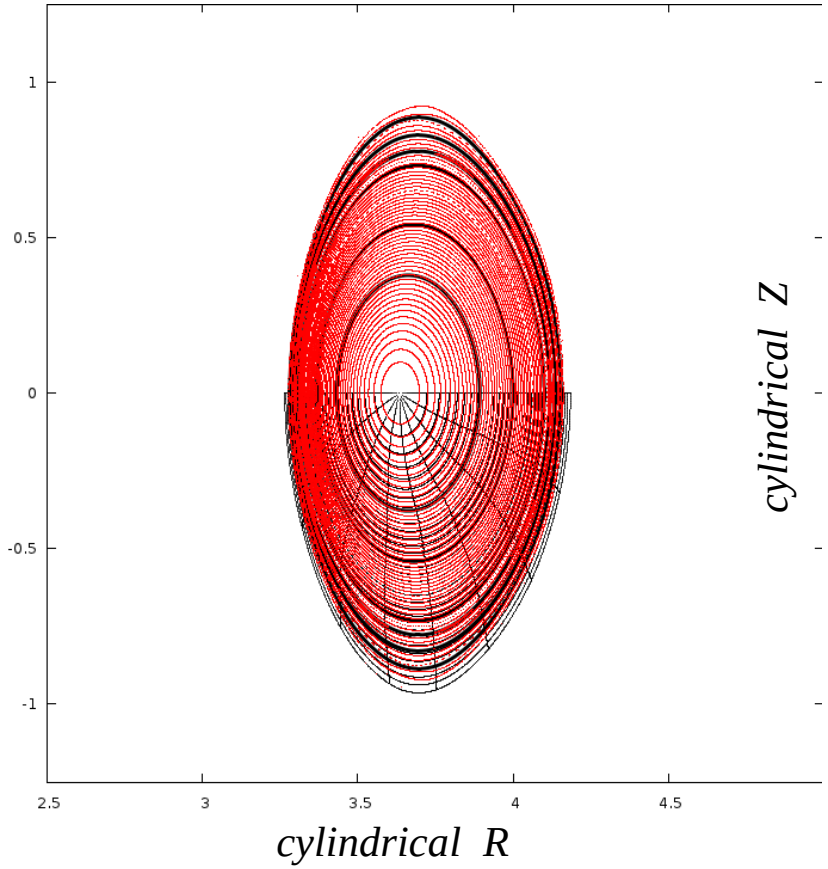

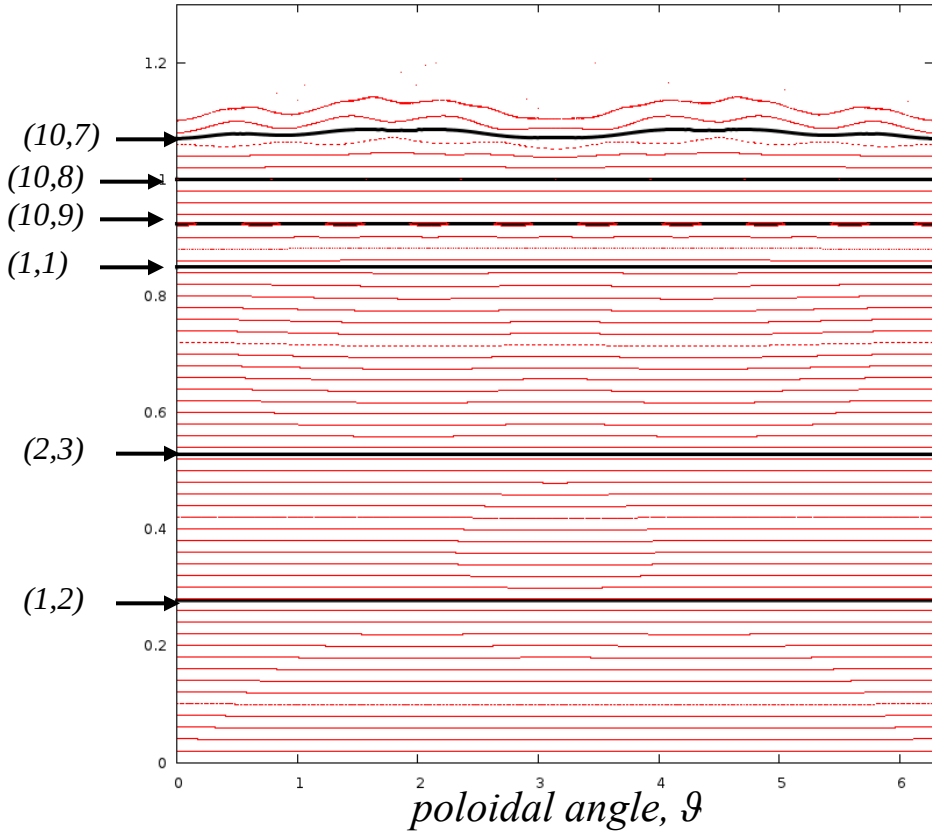

Straight field line coordinates can be constructed over the domain where invariant flux surfaces exist

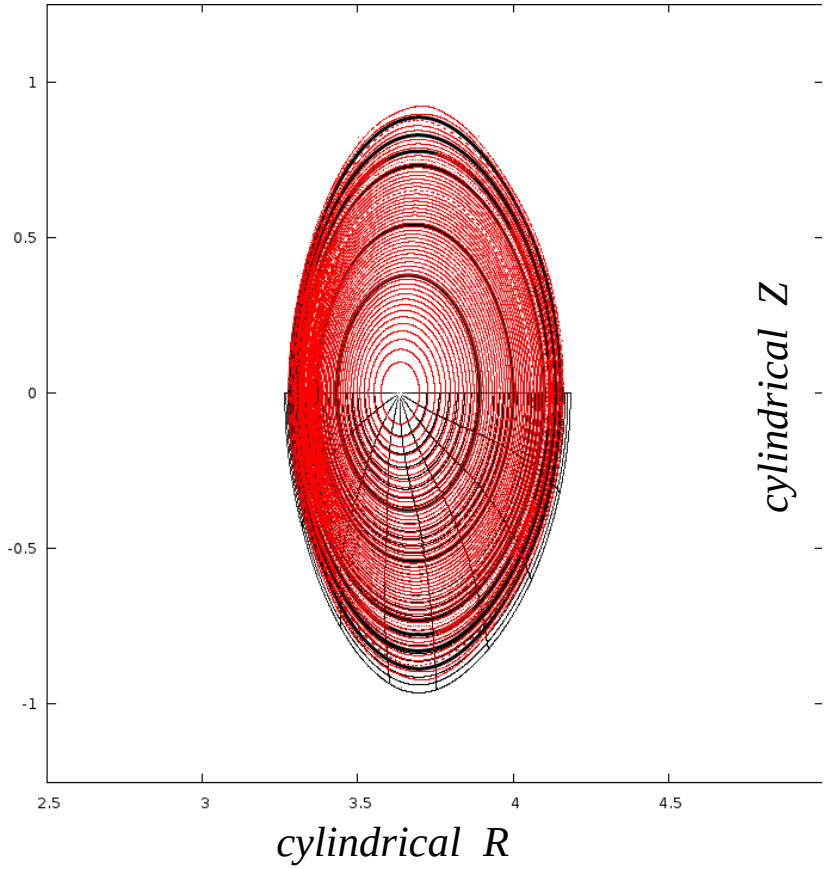

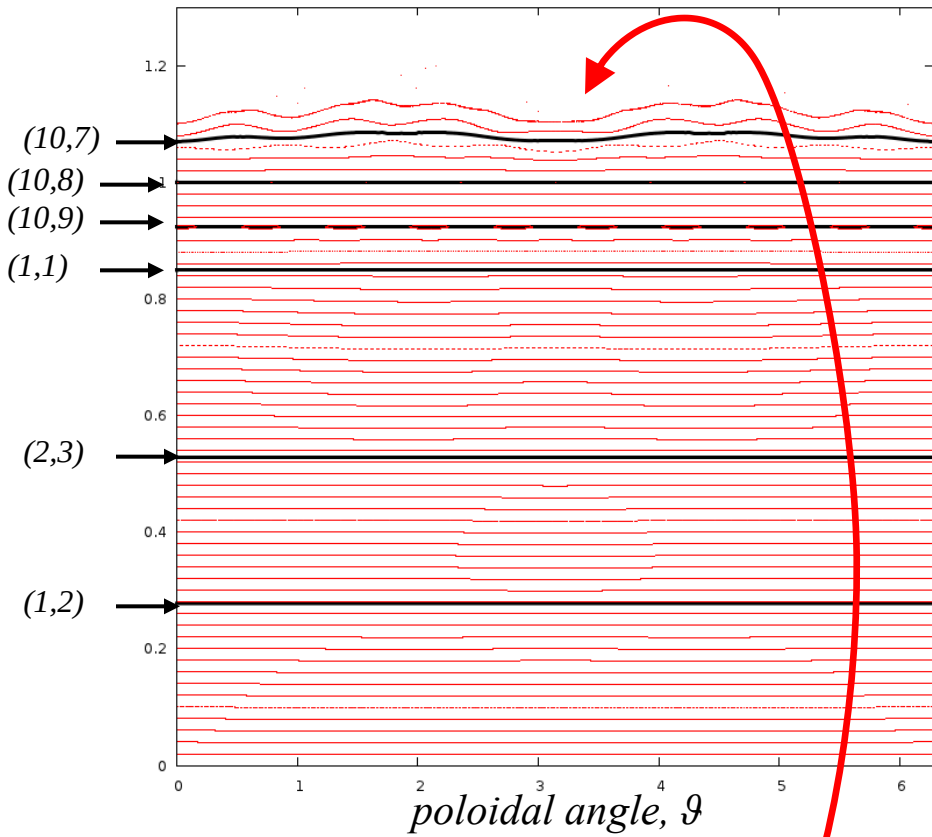

Near the plasma edge, there are magnetic islands, chaotic field lines.
Lets take a closer look . . . . .

Now, examine the “edge” . . . .

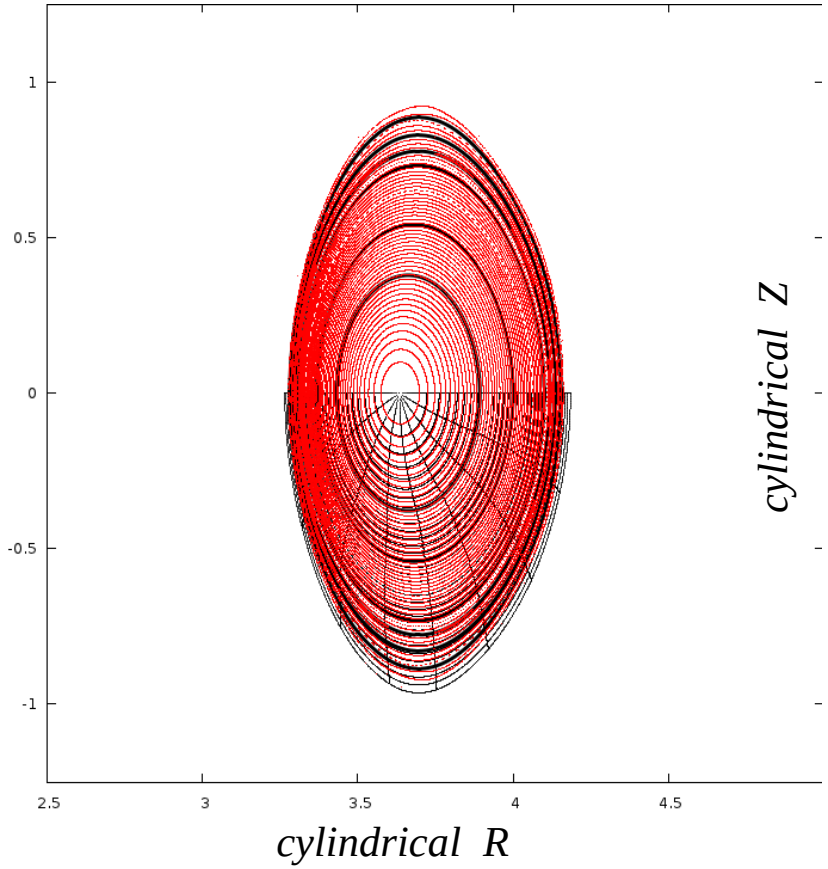

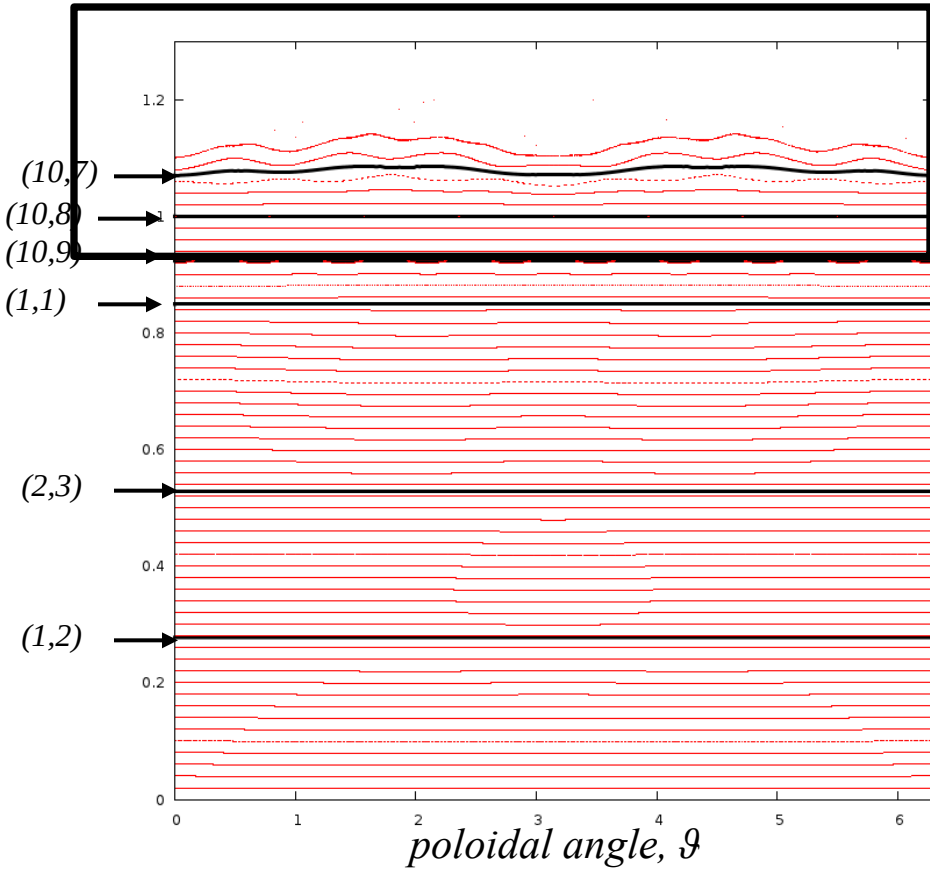

Near the plasma edge, there are magnetic islands and field-line chaos

But this is no problem. There is no change to the algorithm!
The rational, almost-invariant surfaces can still be constructed.
The quadratic-flux minimizing surfaces ≈ ghost-surfaces pass through the island chains,

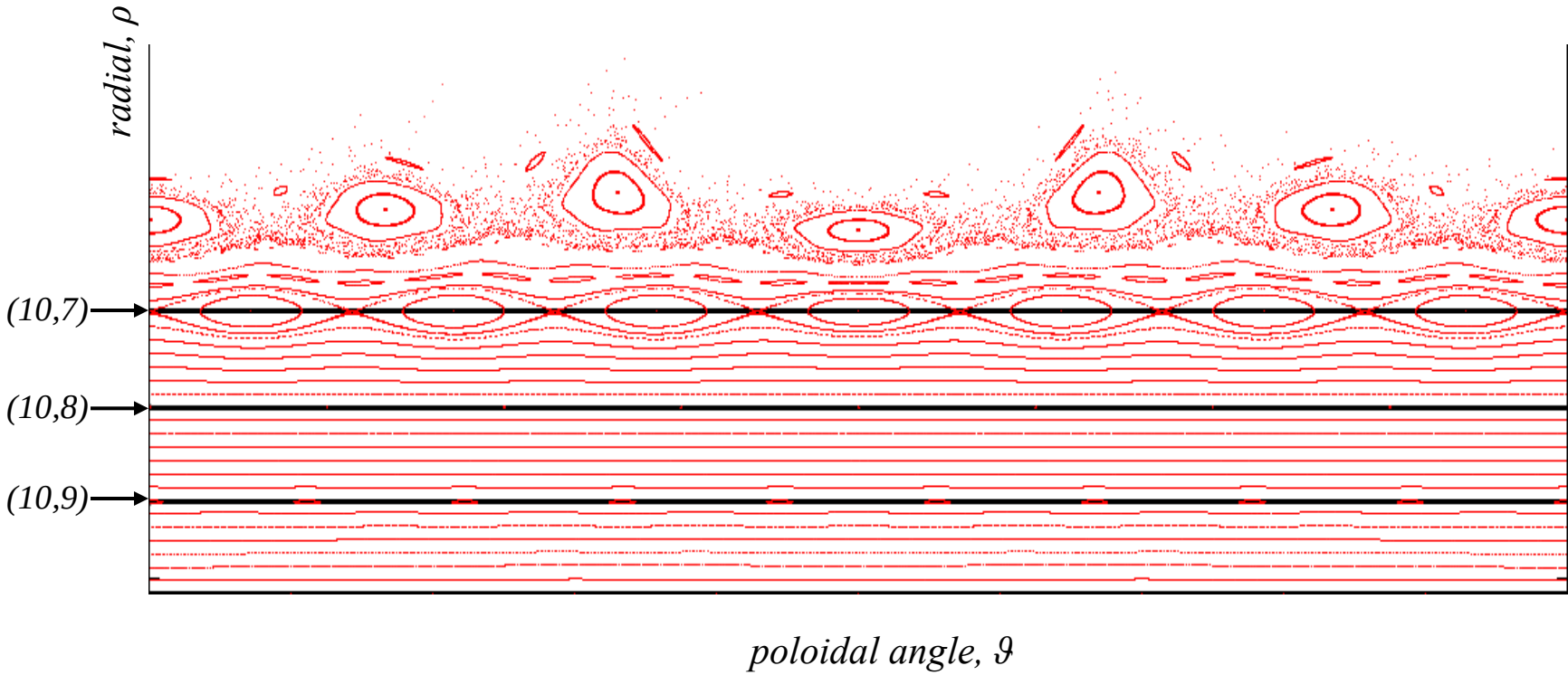

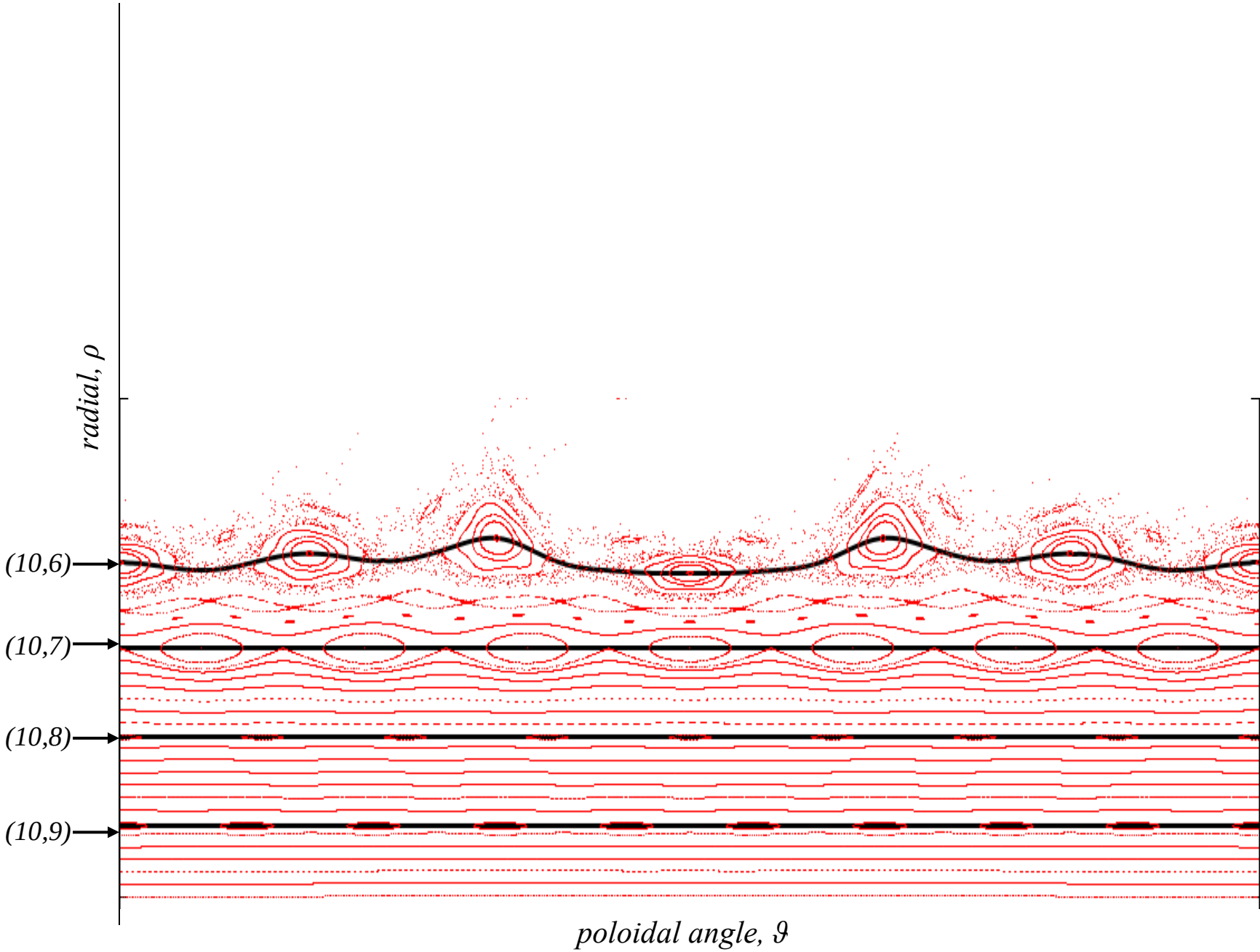
radial, ρ
(10,6)
(10,7)
(10,8)
(10,9)
poloidal angle, ϑ

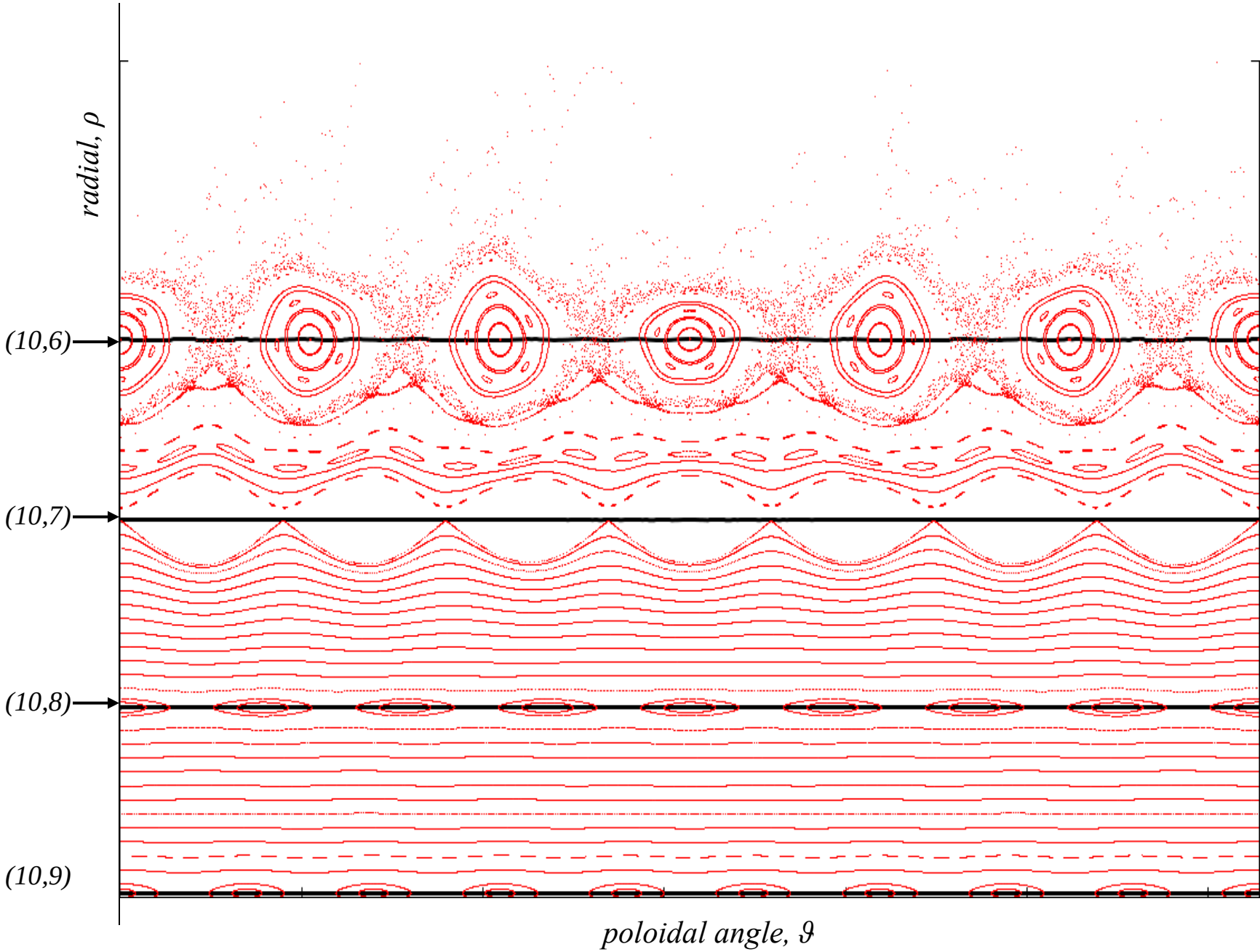
radial, ρ
(10,6)
(10,7)
(10,8)
(10,9)
poloidal angle, ϑ

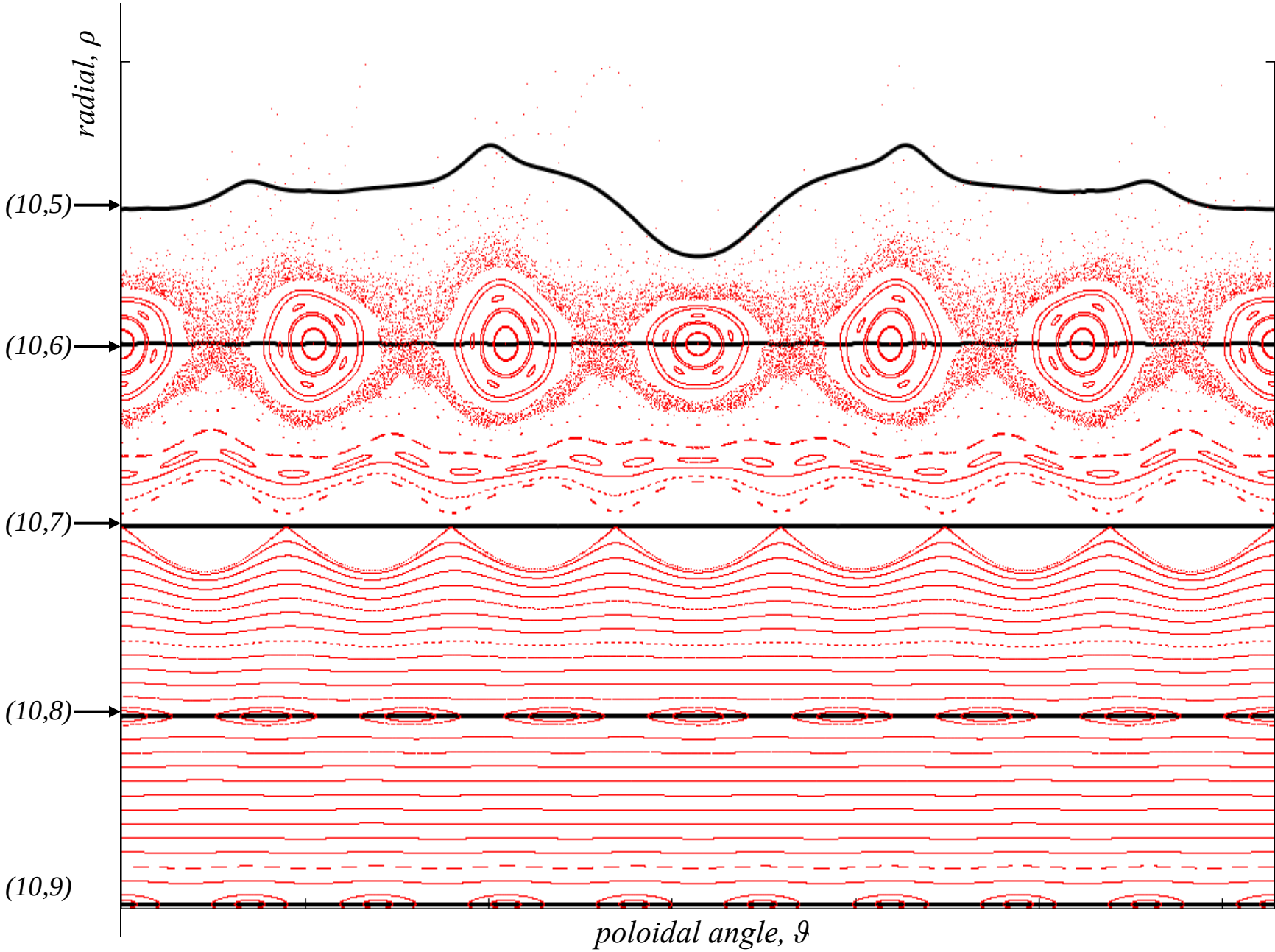
radial, ρ
(10,5)
(10,6)
(10,7)
(10,8)
(10,9)
poloidal angle, ϑ

Now, lets look for the ethereal, last closed flux surface.

(from dictionary.reference.com)
e·the·re·al [ih-**theer**-ee-*uh*l]
Adjective
1.light, airy, or **tenuous**: *an ethereal world created through the poetic imagination.*
2.extremely delicate or refined: *ethereal beauty.*
3.heavenly or celestial: *gone to his ethereal home.*
4.of or pertaining to **the upper regions of space**.

Perhaps the last flux surface is in here

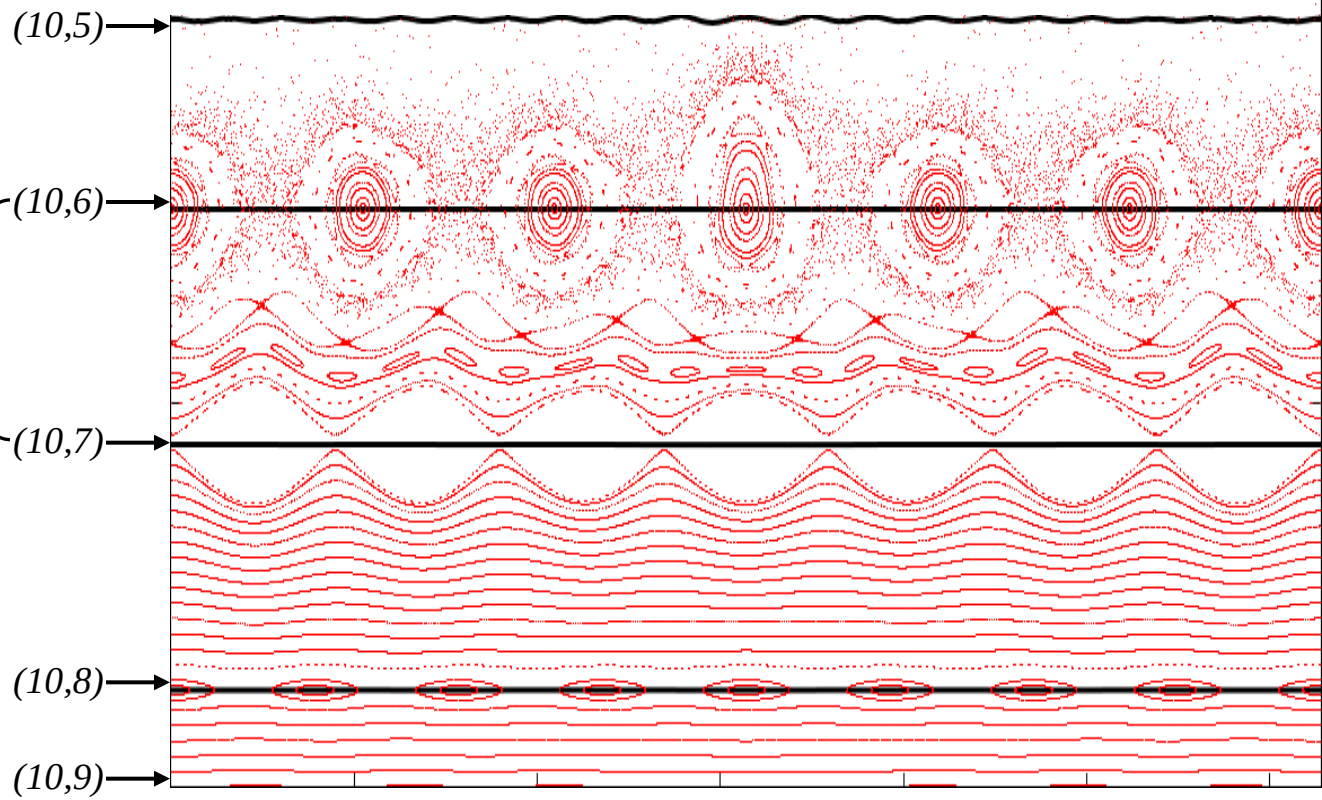

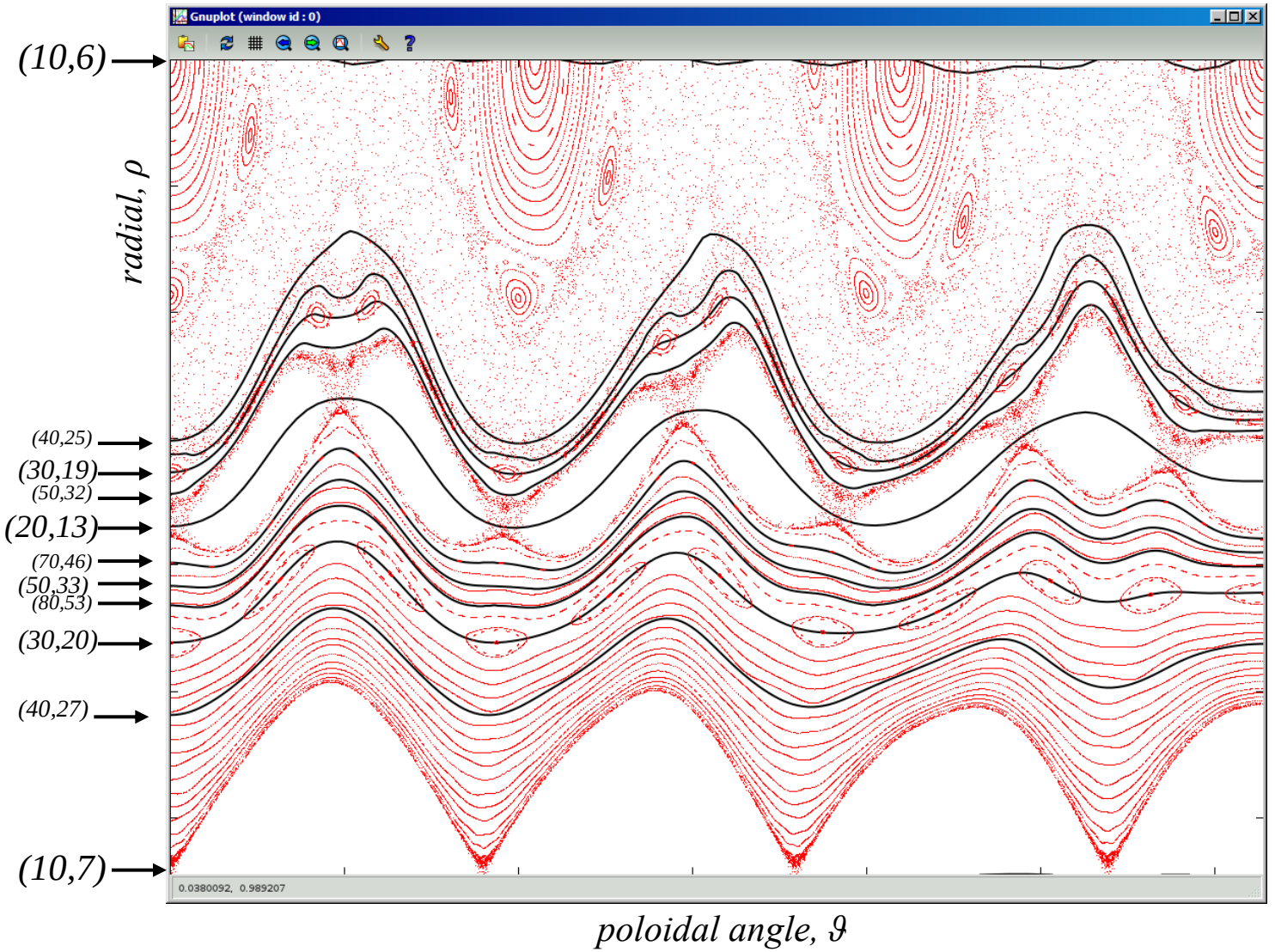

Hereafter, will not Fourier decompose the almost-invariant surfaces and use them as coordinate surfaces.
This is because they become quite deformed and can be very close together,
and the simple-minded piecewise cubic method fails to provide interpolated coordinate surfaces that do not intersect.

(20,13)

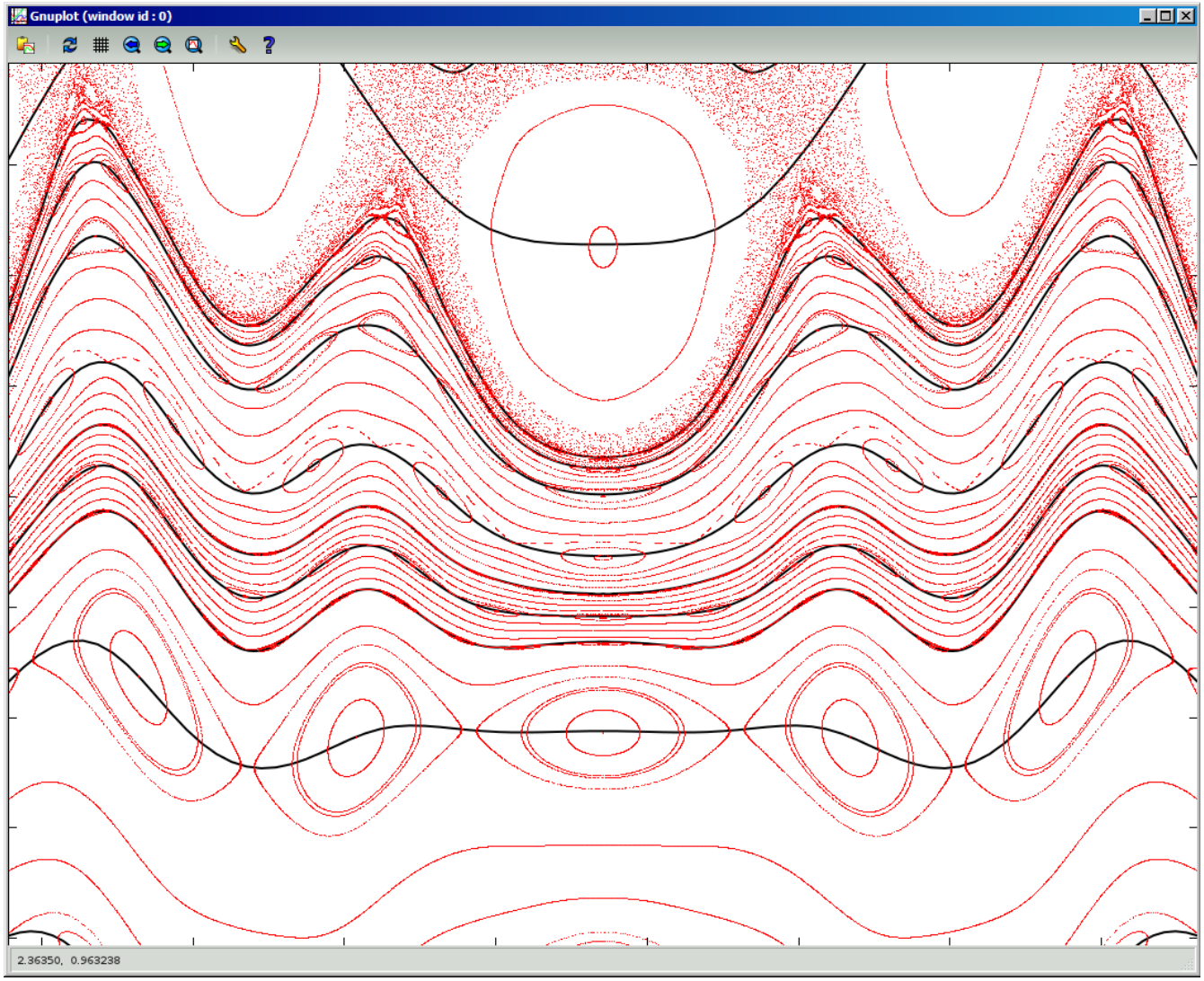

radial, ρ

poloidal angle, ϑ

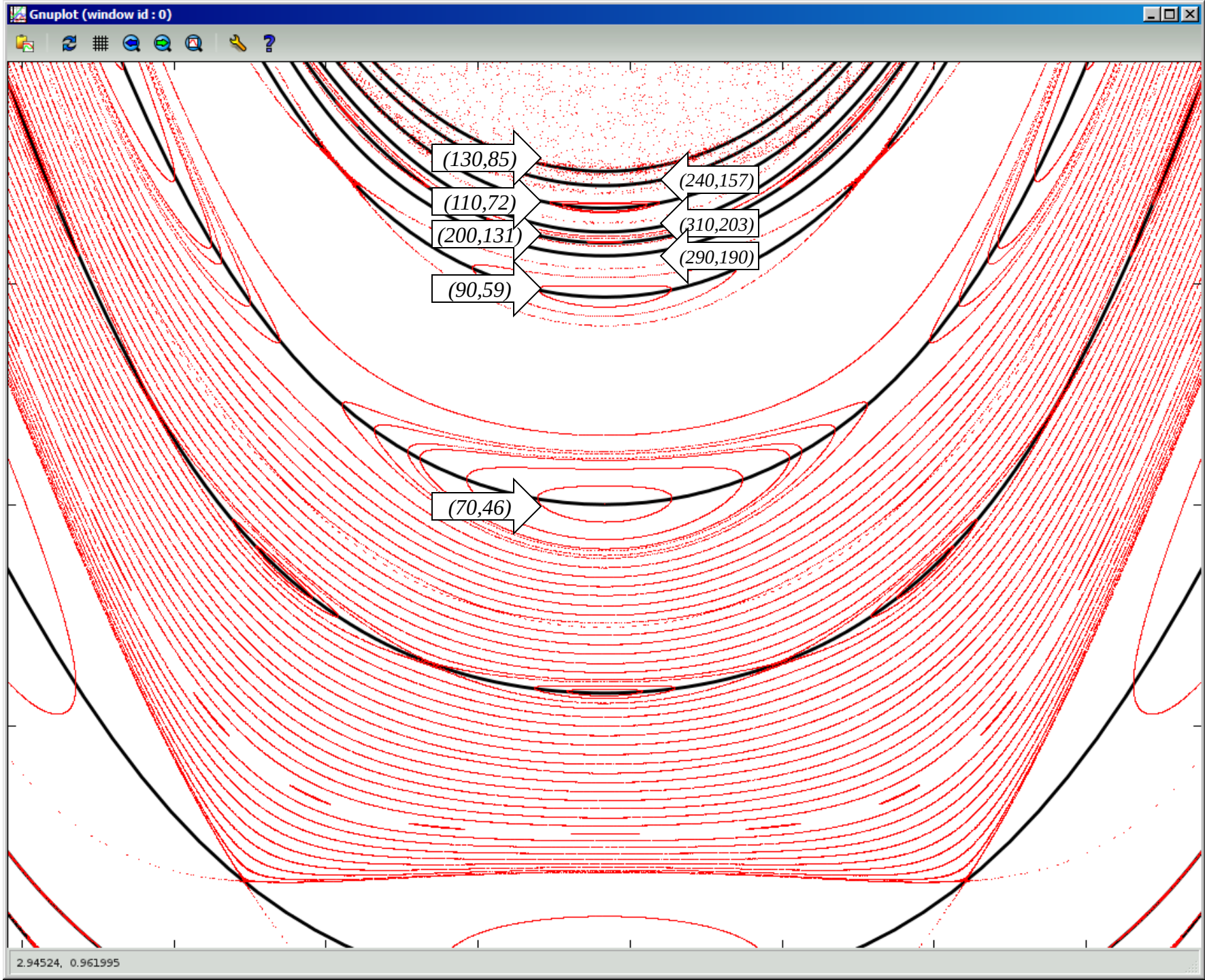
Gnuplot (window id : 0)
(130,85)
(110,72)
(200,131)
(90,59)
(240,157)
(310,203)
(290,190)
(70,46)
2.94524, 0.961995

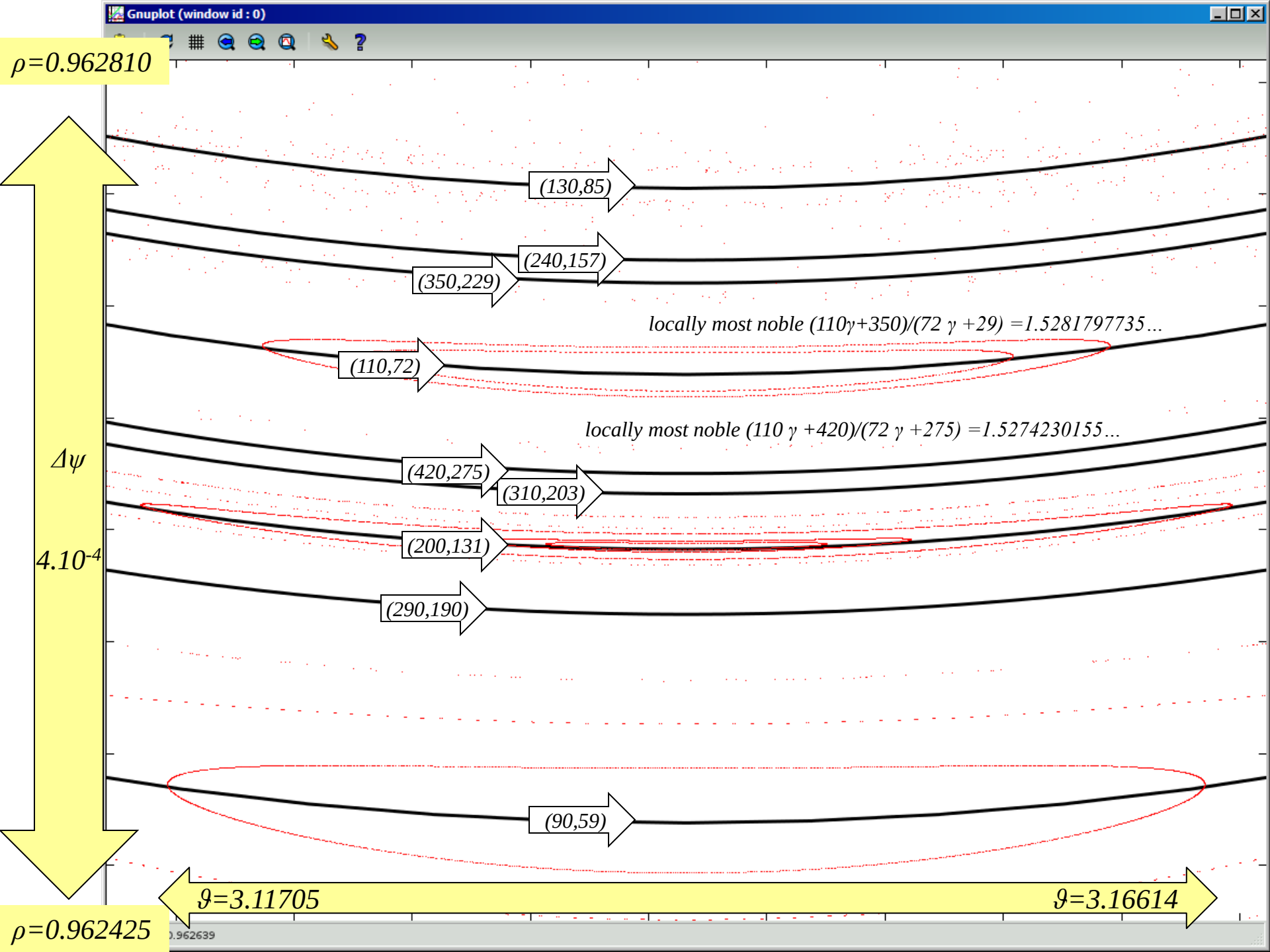
Gnuplot (window id : 0)
ρ=0.962810
(130,85)
(240,157)
(350,229)
locally most noble (110γ+350)/(72 γ +29) =1.5281797735…
(110,72)
locally most noble (110 γ +420)/(72 γ +275) =1.5274230155…
(420,275)
(310,203)
(200,131)
(290,190)
Δψ
4.10-4
(90,59)
ϑ=3.11705
ϑ=3.16614
ρ=0.962425
0.962639

To find the significant barriers to field line transport, construct a hierarchy of high-order surfaces, and compute the upward flux

$\Psi_{10/7}$	7.50156×10^{-04}
$\Psi_{40/27}$	5.35875×10^{-06}
$\Psi_{30/20}$	2.17100×10^{-05}
$\Psi_{110/73}$	5.76470×10^{-08}
$\Psi_{80/53}$	3.18777×10^{-07}
$\Psi_{290/192}$	2.90328×10^{-11}
$\Psi_{210/139}$	5.10028×10^{-10}
$\Psi_{340/225}$	4.32721×10^{-12}
$\Psi_{130/86}$	2.10427×10^{-08}
$\Psi_{180/119}$	2.95639×10^{-09}
$\Psi_{230/152}$	2.23672×10^{-09}
$\Psi_{50/33}$	3.67232×10^{-06}
$\Psi_{120/79}$	7.86600×10^{-08}
$\Psi_{70/46}$	1.37526×10^{-06}
$\Psi_{90/59}$	8.35105×10^{-07}
$\Psi_{290/190}$	6.50293×10^{-08}
$\Psi_{200/131}$	7.07049×10^{-08}
$\Psi_{310/203}$	3.85707×10^{-07}
$\Psi_{420/275}$	3.73482×10^{-07}
$\Psi_{110/72}$	8.62439×10^{-07}
$\Psi_{350/229}$	1.29837×10^{-07}
$\Psi_{240/157}$	4.27556×10^{-07}
$\Psi_{130/85}$	6.22742×10^{-07}
$\Psi_{20/13}$	1.87579×10^{-04}
$\Psi_{90/58}$	4.90660×10^{-06}
$\Psi_{70/45}$	7.79506×10^{-06}
$\Psi_{50/32}$	1.89412×10^{-05}
$\Psi_{80/51}$	7.84026×10^{-06}
$\Psi_{30/19}$	9.25352×10^{-05}
$\Psi_{10/6}$	3.71570×10^{-03}

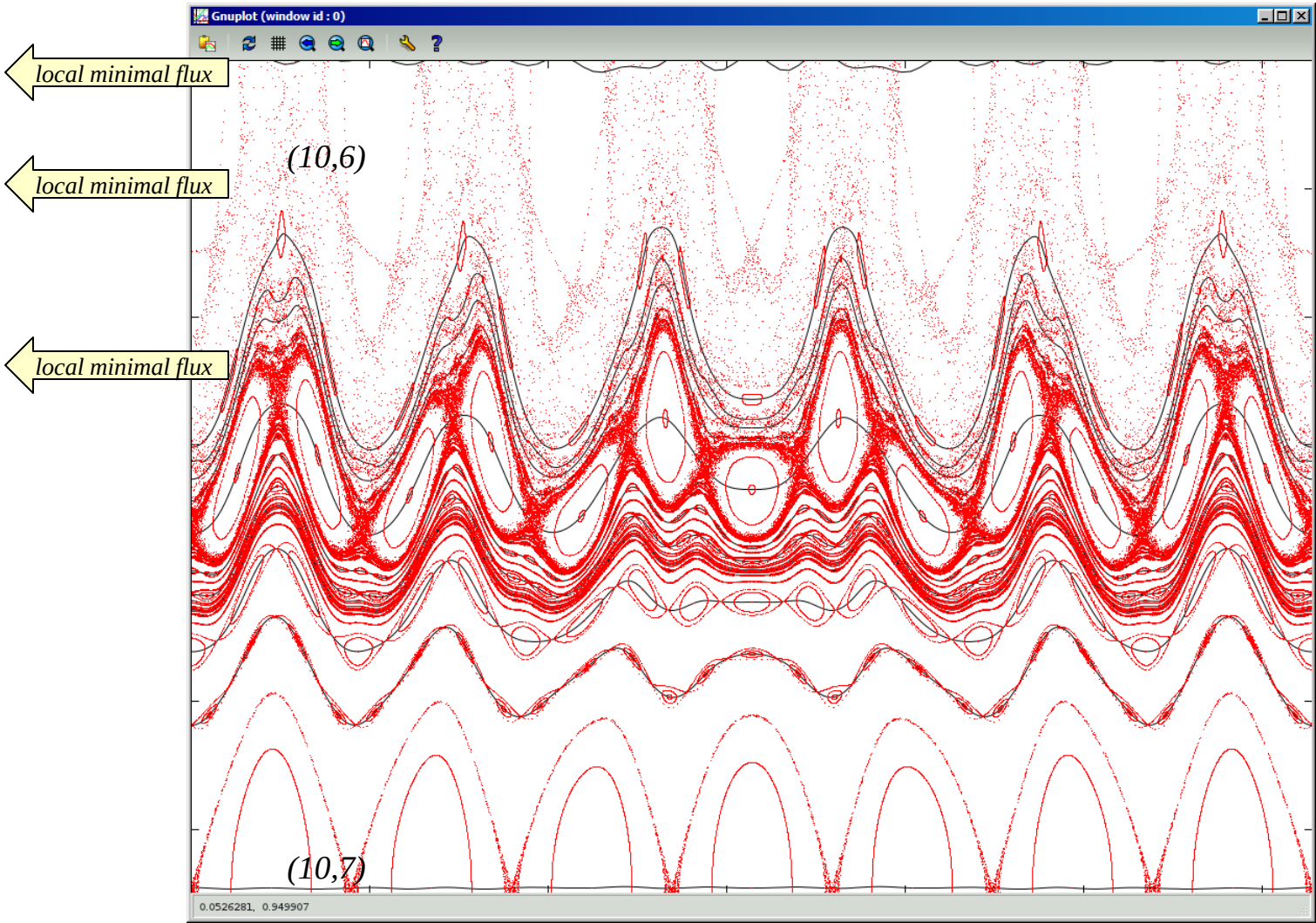

The construction of chaotic coordinates simplifies anisotropic diffusion

$$\frac{\partial T}{\partial t} = \nabla \cdot (\kappa_{\|} \nabla_{\|} T + \kappa_{\perp} \nabla_{\perp} T) + Q,$$

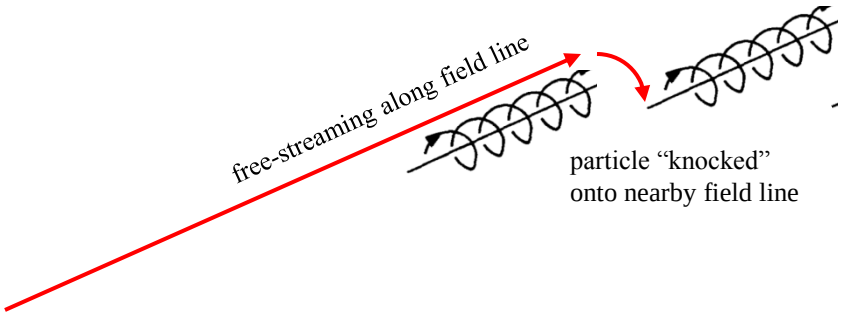

In chaotic coordinates, the temperature becomes a surface function, $T=T(s)$, where s labels invariant (flux) surfaces or almost-invariant surfaces.

If $T=T(s)$, the anisotropic diffusion equation can be solved analytically, $\frac{dT}{ds} = \frac{c}{\kappa_{\|}\varphi + \kappa_{\perp} G}$,

where c is a constant, and

$\varphi = \int\int d\theta d\phi \sqrt{g} B_n^2$, is related to the quadratic-flux across an invariant or almost-invariant surface,

$G = \int\int d\theta d\phi \sqrt{g} g^{ss}$, is a geometric coefficient.

An expression for the temperature gradient in chaotic fields
S.R. Hudson, Physics of Plasmas, 16:010701, 2009
Temperature contours and ghost-surfaces for chaotic magnetic fields
S.R.Hudson and J.Breslau
Physical Review Letters, 100:095001, 2008

When the upward-flux is sufficiently small,
so that the parallel diffusion across an almost-invariant surface is comparable to the perpendicular diffusion,
the plasma cannot distinguish between a perfect invariant surface and an almost invariant surface

Comments

1) Constructing almost-invariant surfaces is very fast, about 0.1sec each surface, and each surface may be constructed in parallel. (In fact, each periodic curve on each surface can be constructed in parallel.)

2) To a very good approximation, the pressure becomes a surface function, $p=p(\rho)$, (where the pressure, temperature satisfy an anisotropic diffusion equation)

3) Chaotic-coordinates are straight-field line coordinates on the periodic orbits (and the KAM surfaces), and

are *nearly* straight field line coordinates throughout the domain (ϑ is linear, ψ is constant).

Eqn(1) $\mathbf{A} = \psi\nabla\theta - \chi(\psi,\theta,\zeta)\nabla\zeta \qquad \chi(\psi,\theta,\zeta) = \chi_0(\psi) + \epsilon\chi_1(\psi,\theta,\zeta) \qquad \begin{aligned} \dot{\theta} &\approx \chi_0'(\psi) \\ \dot{\psi} &\approx 0 \end{aligned}$

1) The last closed flux surface can be determined using a systematic, reliable method, and the upward magnetic-field line flux across near-critical cantori near the plasma edge can be determined. There is not one "plasma boundary". Depending on the physics, there is a hierarchy of "partial boundaries", which coincide with the surfaces of locally minimal flux.

2) Chirikov island overlap estimate is easily estimated from Eqn(1) above, and Greene's residue criterion is easily calculated by the determinant of the Hessian.

List of publications, *http://w3.pppl.gov/~shudson/*

Generalized action-angle coordinates defined on island chains
R.L.Dewar, S.R.Hudson and A.M.Gibson
Plasma Physics and Controlled Fusion, 55:014004, 2013

Unified theory of Ghost and Quadratic-Flux-Minimizing Surfaces
Robert L.Dewar, Stuart R.Hudson and Ashley M.Gibson
Journal of Plasma and Fusion Research SERIES, 9:487, 2010

Are ghost surfaces quadratic-flux-minimizing?
S.R.Hudson and R.L.Dewar
Physics Letters A, 373(48):4409, 2009

An expression for the temperature gradient in chaotic fields
S.R.Hudson
Physics of Plasmas, 16:010701, 2009

Temperature contours and ghost-surfaces for chaotic magnetic fields
S.R.Hudson and J.Breslau
Physical Review Letters, 100:095001, 2008

Calculation of cantori for Hamiltonian flows
S.R.Hudson
Physical Review E, 74:056203, 2006

Almost invariant manifolds for divergence free fields
R.L.Dewar, S.R.Hudson and P.Price
Physics Letters A, 194(1-2):49, 1994

Chaotic coordinates “straighten out” chaos

Poincaré plot of chaotic field
(in **action-angle** coordinates of **unperturbed** field)

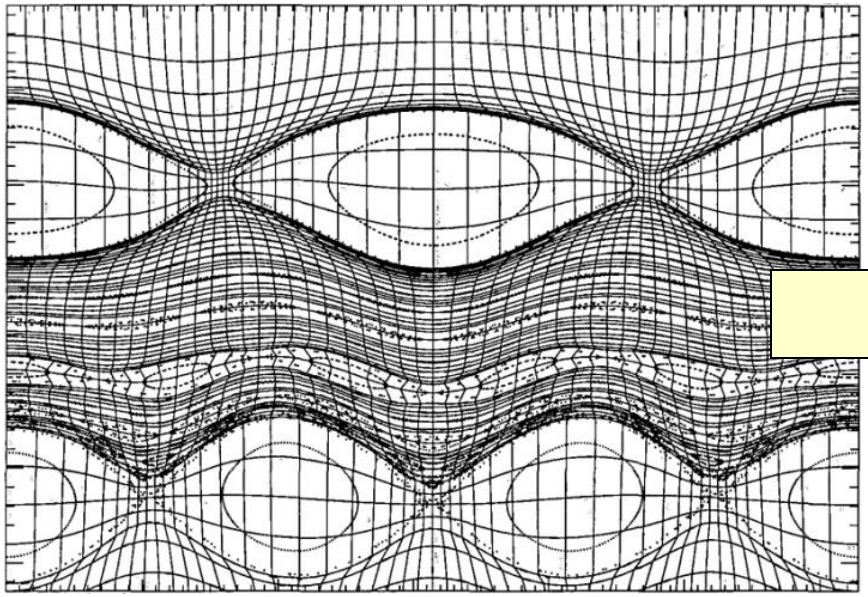

old radial coordinate →

old angle coordinate →

Poincaré plot of chaotic field
in chaotic coordinates

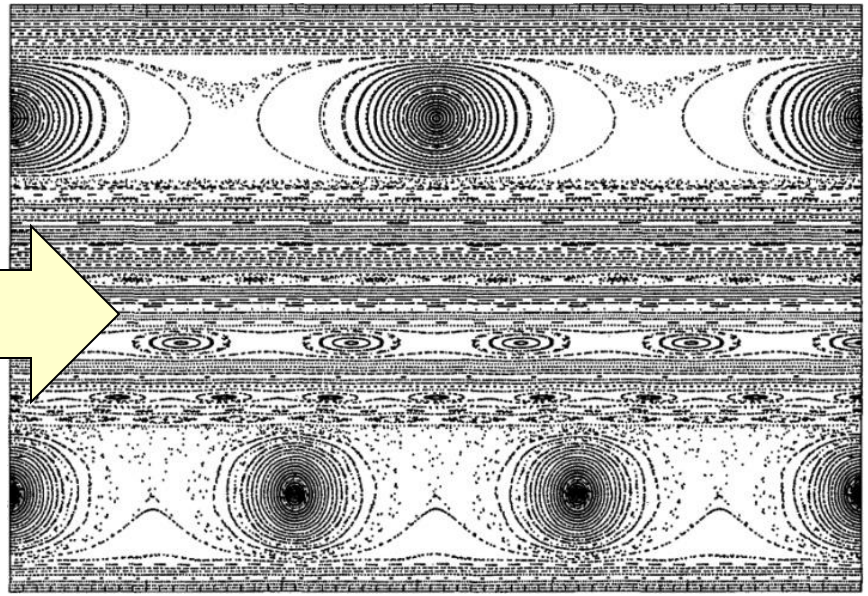

new radial coordinate →

new angle coordinate →

phase-space is partitioned into (1) regular (“irrational”) regions with “good flux surfaces”, temperature gradients
and (2) irregular (“ rational”) regions with islands and chaos, flat profiles

Generalized magnetic coordinates for toroidal magnetic fields
S.R. Hudson, Doctoral Thesis, The Australian National University, 1996

Chaotic coordinates simplify anisotropic transport

The temperature is constant on ghost surfaces, $T=T(s)$

1. Transport *along* the magnetic field is *unrestricted*
→ consider parallel random walk, with **long** steps≈*collisional mean free path*

2. Transport *across* the magnetic field is *very small*
→consider perpendicular random walk with **short** steps≈*Larmor radius*

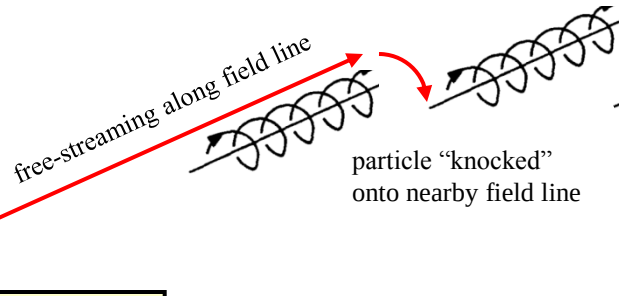

3. Anisotropic diffusion balance $\kappa_{\|}\,\nabla_{\|}^2\,T+\kappa_{\perp}\,\nabla_{\perp}^2\,T=0\,,\quad \kappa_{\|}\gg\kappa_{\perp},\quad \kappa_{\perp}\big/\kappa_{\|}\sim 10^{-10}$

$2^{12}\times 2^{12}=4096\times 4096$ grid points
(to resolve small structures)

4. Compare solution of numerical calculation to ghost-surfaces

5. The temperature adapts to KAM surfaces,cantori,
and ghost-surfaces!
i.e. $T=T(s)$, where s=const. is a ghost-surface

from $T=T(s,\theta,\phi)$ to $T=T(s)$ is a fantastic simplification, allows analytic solution

$$\frac{d\,T}{d\,s}\propto\frac{1}{\kappa_{\|}\,\varphi_2\,+\,\kappa_{\perp}\,G}$$

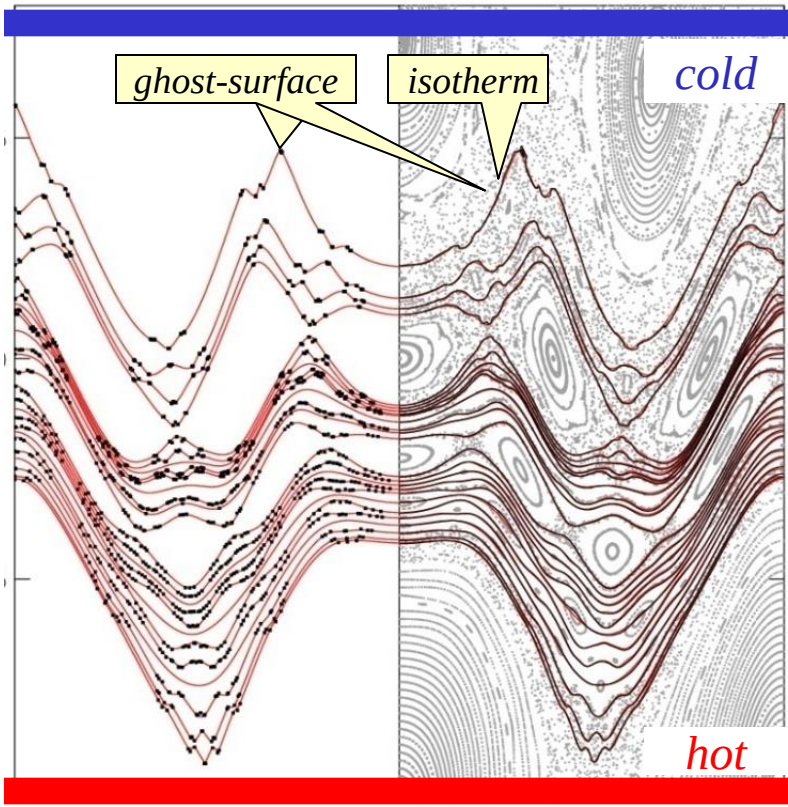

Temperature contours and ghost-surfaces for chaotic magnetic fields
S.R. Hudson et al., Physical Review Letters, 100:095001, 2008
Invited talk 22nd IAEA Fusion Energy Conference, 2008
Invited talk 17th International Stellarator, Heliotron Workshop, 2009

An expression for the temperature gradient in chaotic fields
S.R. Hudson, Physics of Plasmas, 16:100701, 2009